

1 **Stage-specific drivers of Pacific hake (*Merluccius productus*) recruitment in the California**
2 **Current Ecosystem**

3

4 **Running title: Environmental drivers of Pacific hake recruitment**

5

6 Cathleen D. Vestfals^{1*}, Kristin N. Marshall², Nick Tolimieri³, Mary E. Hunsicker⁴, Aaron M.
7 Berger¹, Ian G. Taylor², Michael G. Jacox^{5,6}, and Brendan D. Turley^{7,8}

8

9 **ABSTRACT**

10 Understanding environmental drivers of recruitment variability in marine fishes remains
11 an important challenge in fish ecology and fisheries management. We developed a conceptual
12 life-history model for Pacific hake (*Merluccius productus*) along the west coast of the U.S. and
13 Canada to generate stage-specific and spatiotemporally-specific hypotheses regarding the
14 oceanographic and biological variables that likely influence their recruitment. Our model
15 included seven life stages from pre-spawning female conditioning through pelagic juvenile
16 recruitment (age-0 fish) for the coastal Pacific hake stock. Model-estimated log recruitment
17 deviations from the 2020 hake assessment were used as the dependent variable, with predictor
18 variables drawn primarily from a regional ocean reanalysis for the California Current Ecosystem.
19 Indices of prey and predator abundance were also included in our analysis, as were predictors of
20 local- and basin-scale climate. Five variables explained 59% of the recruitment variability not
21 accounted for by the stock-recruitment relationship in the hake assessment. Recruitment
22 deviations were negatively correlated with May – September eddy kinetic energy between 34.5°
23 and 42.5°N, the North Pacific Current Bifurcation Index, and Pacific herring (*Clupea pallasii*)
24 biomass during the spawner preconditioning stage, alongshore transport during the yolk-sac
25 larval stage, and the number of days between storm events during the first-feeding larval stage.
26 Other important predictors included upwelling strength during the preconditioning stage, the
27 number of calm periods during the first-feeding larval stage, and age-1 hake predation on age-0
28 pelagic juveniles. These findings suggest that multiple mechanisms affect Pacific hake survival
29 across different life stages, leading to variability in population-level recruitment.

30

31

32 **KEYWORDS**

33 California Current, environmental drivers, *Merluccius productus*, Pacific hake, recruitment,
34 ROMS, transport

35

36

37 ¹Fishery Resource Analysis and Monitoring Division, Northwest Fisheries Science
38 Center, National Marine Fisheries Service, National Oceanic and Atmospheric Administration,
39 Newport, OR, USA

40

41 ²Fishery Resource Analysis and Monitoring Division, Northwest Fisheries Science
42 Center, National Marine Fisheries Service, National Oceanic and Atmospheric
43 Administration, Seattle, WA, USA

44

45 ³Conservation Biology Division, Northwest Fisheries Science Center, National Marine
46 Fisheries Service, National Oceanic and Atmospheric Administration, Seattle, WA, USA

47

48 ⁴Fish Ecology Division, Northwest Fisheries Science Center, National Marine Fisheries Service,
49 National Oceanic and Atmospheric Administration, Newport, WA, USA

50

51 ⁵Environmental Research Division, Southwest Fisheries Science Center, National Marine
52 Fisheries Service, National Oceanic and Atmospheric Administration, Monterey, CA, USA

53

54 ⁶Physical Sciences Laboratory, National Oceanic and Atmospheric Administration, Boulder, CO,
55 USA

56

57 ⁷Cooperative Institute for Marine & Atmospheric Studies, University of Miami - Rosenstiel
58 School of Marine and Atmospheric Science, Miami, FL, USA

59

60 ⁸Southeast Fisheries Science Center, National Marine Fisheries Service, National Oceanic and
61 Atmospheric Administration, Miami, FL, USA

62

63 * Correspondence

64 Cathleen D. Vestfals, Oregon Department of Fish and Wildlife, Newport, OR 97365, USA

65 E-mail: Cathleen.D.Vestfals@odfw.oregon.gov

66

67 This manuscript adheres to the ethics and integrity policies of Fisheries Oceanography.

68

69 **1 | INTRODUCTION**

70 For over a century, there has been intense scientific interest and research effort to identify
71 the factors that influence recruitment variability in marine fishes. Year-class strength is thought
72 to be set during the early larval stage, with recruitment (defined herein as individuals reaching
73 age-1) being linked to number of factors, including first-feeding success ('Critical Period'
74 hypothesis, Hjort, 1914, 1926), transport of eggs and larvae by ocean currents ('Aberrant Drift'
75 hypothesis, Hjort, 1914), match in the timing between larval production and prey resources
76 ('Match-Mismatch' hypothesis, Cushing, 1974, 1990), aggregation of prey via vertical
77 stratification ('Stable Ocean' hypothesis, Lasker, 1978, 1981), and size-based predation ('Stage-
78 Duration' hypothesis, Houde, 1987; Anderson, 1988), among others. To this day, understanding
79 the mechanisms underlying recruitment variability remains a challenge in fish ecology and
80 fisheries management. However, it is clear that the processes and mechanisms that generate
81 recruitment variability work across multiple life stages (Houde, 2008) and that multi-hypothesis,
82 integrative, and interdisciplinary approaches are needed (Hare, 2014).

83 Pacific hake (*Merluccius productus*), also known as Pacific whiting, is an ecologically
84 important species that plays a key trophic role as both predator and prey in the California Current
85 Ecosystem (CCE) (Ressler et al., 2007). Pacific hake occur primarily from the Gulf of California

86 (~25°N) to the Gulf of Alaska (~55°N) (Figure 1), occupying southern waters during the winter
87 spawning season and migrating northward to feed between northern California and northern
88 British Columbia during the spring, summer, and fall when the fishery is conducted (Grandin et
89 al., 2020). Since the stock spans U.S. and Canadian waters, the hake fishery has been
90 cooperatively managed through a bilateral agreement between the two countries since 2011, with
91 quotas based on a harvest control rule and a fixed allocation share of the annual total allowable
92 catch to each country (Jacobsen et al., 2019). Pacific hake population dynamics are strongly
93 influenced by the periodic appearance of strong cohorts that have occurred across a range of
94 population sizes (Figure 2). The stock assessment suggests that recruitment is highly variable
95 (Figure 2b), resulting in large and rapid biomass changes, but the mechanisms underlying this
96 variability are poorly understood. As a result, estimates of stock status and stock trajectory
97 projections for Pacific hake remain highly uncertain due to the variability and uncertainty in the
98 recruitment estimates, as cohort strength is generally not well detected until age 3 or 4 (Berger et
99 al., 2019). Given the weak stock-recruitment relationship estimated by the stock assessment
100 model (Figure 2c), environmental factors that vary at multiple spatial and temporal scales, such
101 as temperature and upwelling strength, are likely important (Bailey, 1981).

102 Understanding the linkage between Pacific hake population dynamics and environmental
103 conditions has been identified as a high priority research need for improving stock assessments
104 and hake management strategies (Berger et al., 2019). Focusing on the survival of early life-
105 history stages may be especially informative, as recruitment variability is known to have a
106 stronger influence on the performance of alternative management strategies than rates of
107 movement or the spatial distribution of the population (Jacobsen et al., 2019).

108 Initial research into the causes of Pacific hake recruitment variability began in the 1980s.
109 Bailey and Francis (1985) linked recruitment of age-3 Pacific hake to post-larval abundance off
110 the California coast in spring, suggesting that year-class strength was set during the first year of
111 life. During the 1970s, recruitment strength was negatively correlated with temperature and
112 upwelling (Bailey, 1981). However, these relationships did not persist in the 1980s (Bailey and
113 Francis, 1985). More recently, Horne and Smith (1997) noted that changes in larval hake
114 biomass were dominated by mortality and drift with prevailing currents, while Lo (2007) found
115 that decreased larval production was associated with increasing ocean temperature since the
116 1980s. Strong year classes of Pacific hake and several other gadoid stocks have been linked to
117 conditions related to the El Niño-Southern Oscillation (ENSO), which suggests that large-scale
118 climate drivers play an important role (Hollowed et al., 2001). Factors that regulate larval
119 delivery to nursery habitats, such as variation in circulation and mortality of eggs and larvae, are
120 known to influence year-class strength (Houde, 2008; Rijnsdorp et al., 1995; Van der Veer et al.,
121 2000), and transport has been linked to year-class formation in several Northeast Pacific marine
122 fishes (Bailey et al., 1982; Vestfals et al., 2014; Wilderbuer et al., 2002). Species like Pacific
123 hake may be especially sensitive to variations in climate due to their spatially separated
124 spawning locations, nursery areas, and adult feeding grounds, which require the active migration
125 of adults and ocean currents to transport eggs and larvae to complete their life cycle (“Migration
126 Triangle” hypothesis, Harden Jones, 1968).

127 Technological advances in the last several decades have increased our ability to explore
128 relationships between oceanic and atmospheric processes and fish populations. For example,
129 monthly composite satellite sea surface temperature (SST) and surface chlorophyll *a* data have
130 been used to predict potential spawning habitat of northern anchovy (*Engraulis mordax*) and

131 Pacific sardine (*Sardinops sagax*) in the CCE (Reiss et al., 2008), while maps of sea surface
132 height (SSH) constructed from satellite observations of sea level anomaly have shown that white
133 sharks (*Carcharodon carcharias*) exhibit a clear affinity for mesoscale eddies (Gaube et al.,
134 2018). Atmospheric and oceanic reanalysis products and ocean circulation models have been
135 used to examine how oceanographic and atmospheric processes affected recruitment variability
136 and productivity in several Northeast Pacific marine fish populations (Haltuch et al., 2020;
137 Litzow et al., 2018; Malick et al., 2017; Tolimieri et al., 2018; Vestfals et al., 2014).
138 Technological developments such as these provide a unique opportunity to revisit hypotheses
139 about the physical and biological processes that determine Pacific hake year-class strength
140 developed in the 1980s, and can potentially help to identify earlier indicators of recruitment
141 strength (i.e., age-1) than are currently available (i.e., age-3 or -4).

142 In this study, we (i) developed a literature-based, conceptual life-history model for
143 Pacific hake in the CCE that included seven stages from the conditioning of pre-spawning
144 females through the pelagic juvenile phase (age-0 fish) for the U.S. west coast Pacific hake
145 stock; (ii) used our conceptual model to generate stage-, space-, and time-specific hypotheses
146 regarding the physical and biological variables that likely influence Pacific hake recruitment; and
147 (iii) developed and compared several linear models to predict Pacific hake recruitment using
148 oceanographic variables derived from a regional ocean reanalysis for the CCE (Neveu et al.,
149 2016). We also investigated how biological indices like predator and prey abundances and local-
150 and basin-scale climate drivers (as proxies for nutrient input or changes in ocean currents) might
151 affect Pacific hake recruitment. Our analysis re-examined existing hypotheses of where and
152 when year-class strength is determined and investigated the relationships between ocean
153 conditions and Pacific hake survival across early life-history stages leading to recruitment, with

154 the goal of improving our understanding of the drivers of hake recruitment variability.

155

156 **2 | METHODS**

157 To address our objectives, we applied the methodology used by Tolimieri et al. (2018) for
158 sablefish (*Anoplopoma fimbria*) and Haltuch et al. (2020) for petrale sole (*Eopsetta jordani*) to
159 the U.S. west coast Pacific hake stock. We used estimates of log recruitment deviations from the
160 2020 hake stock assessment (Grandin et al., 2020) and model output from a CCE configuration
161 of the Regional Ocean Modeling System (ROMS) with data assimilation (Neveu et al., 2016).

162 The stock assessment model is an age-structured model fit to an acoustic survey index of
163 biomass, annual catch data, and age-composition data from the survey and commercial fisheries
164 (more details can be found in Grandin et al., 2020). Recruitment is estimated using a Beverton-
165 Holt stock-recruitment relationship where the unexploited recruitment parameter is freely
166 estimated and steepness is estimated using a weakly informative prior. The year-specific
167 deviations are estimated using a fixed standard deviation of 1.4. Although recruitment estimates
168 from the Pacific hake stock assessment were available from 1966 – 2019, our analysis was
169 constrained to the 1980 – 2010 period for which a self-consistent, high-resolution regional ocean
170 reanalysis was available to provide three-dimensional oceanographic conditions (see Section
171 2.2.1). We focused on the reproductively-active portion of the stock (U.S. west coast) occurring
172 within the region encompassed by the ROMS model, although variables representing conditions
173 outside of this region were incorporated into our analysis from other sources. We considered the
174 time from pre-spawning female conditioning through age-0 pelagic juveniles. By using this
175 conceptual approach, we were able to generate stage-specific and spatiotemporally-specific
176 hypotheses regarding the physical and biological variables likely to influence Pacific hake

177 survival at each life stage leading to recruitment. We tested our hypotheses using linear
178 modeling, model selection, and model validation.

179

180 **2.1 | Pacific hake life history: Female preconditioning to age-0 recruits**

181 Our conceptual life-history model began by first identifying each stage in the life history
182 of Pacific hake where environmental drivers might impact the size of each year class, beginning
183 with female conditioning prior to the spawning season through age-0 pelagic juveniles (Tables 1
184 and A1). Female condition has generally been shown to influence whether or not an individual
185 spawns, the quality and number of eggs that are produced, as well as their hatching success
186 (Laine & Rajasilta, 1999; Rodgveller et al., 2016; Sogard et al., 2008). Adult Pacific hake are
187 found throughout the water column in association with the shelf break, typically over bottom
188 depths ranging between 100 m and 300 m (Bailey et al., 1982; Cooke et al., 2006; Ressler et al.,
189 2007). Their northward feeding migration is timed with the spring transition in ocean conditions
190 along the shelf edge (Benson et al., 2002; Thompson, 1981). Adult Pacific hake spend summers
191 feeding off the coasts of Oregon, Washington, and British Columbia before migrating southward
192 in autumn to their spawning grounds off central and southern California, and Baja California,
193 Mexico (Hollowed & Bailey, 1989). Thus, the feeding period from spring to fall (April to
194 October) prior to spawning was considered important for female preconditioning.

195 Pacific hake are believed to spawn during the winter months, mainly between December
196 and March (Smith, 1995), with the peak occurring in January and February (Bailey, 1980;
197 Stauffer, 1985; Woodbury et al., 1995). While the exact location is unknown, spawning is
198 thought to occur up to 400 km offshore of the southern California Bight at depths of 130 – 500 m
199 over the continental slope (Bailey et al., 1982; Nelson & Larkins, 1970; Tillman, 1968), though

200 several studies have noted that hake spawning grounds are not fixed, but rather variable in
201 location (Agostini et al., 2006; Horne & Smith, 1997; Sakuma & Ralston 1997).

202 After spawning, eggs rise upwards to the depth of neutral buoyancy, usually to the base
203 of the mixed layer (Bailey et al., 1982). Time to hatch varies with temperature, but is typically
204 around 4 to 5 days (Bailey, 1982). Both eggs and larvae are often found aggregated near the base
205 of the mixed layer, usually at about 40 – 60 m depth (Ahlstrom, 1959; Bailey et al., 1982). Most
206 early-stage larvae are found between January and March, with a peak in February (Hollowed,
207 1992). Yolk-sac larvae are mostly found at depths between 50 – 100 m, with yolk sac absorption
208 occurring at 4.0 mm (Cass-Calay, 1997), when larvae are approximately 10 days old (Bailey &
209 Francis, 1985), though this may occur earlier at higher temperatures (Bailey, 1982). First-feeding
210 larvae (> 4.0 mm) can be found from 50 – 200 m deep over the continental shelf and slope
211 (Bailey 1981, 1982). Flexion occurs at 10 mm in length (Matarese et al., 1989) after which post-
212 flexion larvae can be found deeper in the water column, between 200 – 500 m during the day, but
213 close to the surface at night, between 25 – 50 m (Bailey, 1982). Transformation to pelagic
214 juveniles occurs between 30 – 35 mm in length (Matarese et al., 1989), with age-0 fish caught in
215 surveys from mid-May to mid-June in the upper mixed layer over the shelf, inshore of the 200-m
216 isobath (Sakuma & Ralston, 1997).

217

218 **2.2 | Generating hypotheses about potential recruitment drivers**

219 We developed *a priori*, life-stage-specific and spatiotemporally-specific (considering
220 time, depth, latitude, and longitude) hypotheses for environmental covariates that may drive
221 recruitment variability in Pacific hake (Tables 1 and A1). Our analysis included covariates
222 obtained from a ROMS model, predator and prey indices, as well as local- (e.g., storm and calm

223 events, SSH) and basin-scale indices representing the El Niño-Southern Oscillation (ENSO), the
224 Pacific Decadal Oscillation (PDO) (Mantua et al., 1997), the North Pacific Gyre Oscillation
225 (NPGO) (Di Lorenzo et al., 2008), and the North Pacific Current (NPC) Bifurcation Index (BI)
226 (Malick et al., 2017). A number of hypotheses were represented by two or more predictors that
227 represented different spatial regions (e.g., cross-shelf transport and upwelling north and south of
228 Point Conception) and several predictors were hypothesized to act on multiple life stages (e.g.,
229 ENSO during the preconditioning, larval, and juvenile stages, euphausiid prey availability during
230 the late larval and pelagic juvenile stages). Thus, a total of 88 predictors were tested.

231 For each hypothesis, we specified the time period, depth, and latitudinal and longitudinal
232 extent of the potential predictor based on the traditional model of hake life history. For example,
233 net cross-shelf transport between January and March, at 40 – 60 m depth, between 31°N and
234 34.5°N, and near the shelf break (defined as being between the 100- and 2,000-m isobaths) may
235 affect the transport and distribution of Pacific hake eggs (Tables 1 and A1). In some cases, the
236 literature suggested multiple potential depth ranges over which environmental variables might
237 influence recruitment. For example, Ahlstrom and Counts (1955) reported that Pacific hake eggs
238 were found between 27 and 140 m while Bailey et al. (1982) reported aggregations of eggs just
239 below the base of the mixed layer, usually at about 40 – 60 m depth. When selecting which
240 environmental predictors to include in model selection, we initially evaluated variables (e.g., net
241 cross-shelf transport) over both the broader and the more restricted depth range. Preliminary
242 analyses showed that these paired predictors were highly correlated (e.g., $r > 0.87$ for the egg
243 stage). We chose to include the narrower depth range version of each in our analyses to reduce
244 the number of predictors because we believed this range more accurately captured the position of
245 eggs and larvae located at the base of the mixed layer. The resulting testable hypotheses fall into

246 six general categories, which may overlap life-history stages (Tables 1 and A1): temperature,
247 transport, mixing, prey, predators, and bottom-up ecosystem processes.

248

249 **2.2.1 | Regional Ocean Model**

250 *Oceanographic information*

251 The majority of the predictors in our analysis were physical oceanographic parameters
252 (e.g., temperature, alongshore and cross-shelf currents, and mixed layer depth), which were
253 derived from the data-assimilative CCE ROMS output (Neveu et al., 2016). The CCE-ROMS
254 model domain covers the region from 30°N – 48°N and from the coastline to 134°W at 0.1° (~10
255 km) horizontal resolution, with 42 terrain-following vertical levels. We used the 1980 – 2010
256 CCE reanalysis, which assimilates satellite observations (SST, SSH) and *in situ* data
257 (temperature and salinity from ships, floats, moorings, gliders) into the model to more accurately
258 represent the true ocean state. This reanalysis has been used extensively in the CCE to study
259 climate-ocean dynamics (Jacox et al., 2014, 2015), bottom-up controls on primary production
260 (Jacox et al., 2016), oceanographic influences on species distributions (Becker et al., 2019;
261 Brodie et al., 2018), and recruitment (Haltuch et al., 2020; Tolimieri et al., 2018). All ROMS
262 output was averaged in 4-day increments and then either averaged or summed over the
263 appropriate period, latitude/longitude, and depth (as defined in Tables 1 and A1) for each of the
264 30 years (n = 30 for each time series in the analysis; see Section 2.4, below).

265 The paucity of subsurface oceanographic data was the motivation for using the CCE
266 ROMS model output in this study. Despite our inability to validate the subsurface model
267 transport, the output provides a physically consistent estimate of subsurface dynamics, though it
268 likely deviates from nature more at the subsurface than at the surface. Data assimilation was used

269 to improve models that already capture the dynamics in the CCE without data assimilation. The
270 model's skill has been extensively documented for applications with and without data
271 assimilation (e.g., Jacox et al., 2015; Veneziani et al., 2009). The model exhibits realistic
272 physical variability even in the absence of data assimilation, as it is forced by realistic winds,
273 surface heat fluxes, and lateral boundary conditions. Further details on the impact of assimilated
274 data on different metrics of the CCE can be found in Moore et al. (2017).

275

276 **2.2.1.1 | Temperature**

277 Temperature may affect Pacific hake recruitment through a number of mechanisms. For
278 example, higher temperatures during the spawning female preconditioning stage (Tables 1 and
279 A1, hypothesis 1 (H1)) may increase energetic demands, causing less energy to be allocated to
280 reproduction, resulting in reduced egg production or potentially skipped spawning. Temperature
281 can also influence the timing and location of spawning, as well as the growth, development, and
282 survival of eggs, larvae, and juveniles through multiple mechanisms. For example, growth rates
283 may be higher at warmer temperatures, which may reduce the time spent by slow-growing and
284 small larvae in stages vulnerable to predation (e.g., the 'Stage-Duration' or 'bigger-is-better'
285 hypotheses; Houde, 1987, 1997). However, metabolic demands may also increase with
286 increasing temperature, making larvae more susceptible to starvation, especially if warmer
287 waters are associated with poor feeding conditions (e.g., lower quality prey or less abundant
288 prey). Modeled temperatures were obtained from the ROMS output. In most cases, we included
289 temperature as degree days (cumulative temperature above a threshold value, Chezik et al.,
290 2014), setting a standard threshold temperature of 5.0°C (Chezik et al., 2014).

291

292 **2.2.1.2 | Transport**

293 Marine species with pelagic eggs and larvae must rely on transport and their own
294 behavior to move them toward and keep them within suitable nursery habitat for successful
295 recruitment to the juvenile stage. Transport to nursery habitat was characterized by ROMS
296 estimates of mean alongshore and cross-shelf transport at specific depths and times for each
297 relevant Pacific hake life history stage (Tables 1 and A1).

298 Pacific hake eggs rise to the base of the mixed layer after spawning (Bailey et al., 1982).
299 Thus, the mixed-layer depth (MLD) may influence how high eggs rise in the water column,
300 which in turn, may affect their transport (Hinckley et al., 1996; Sundby, 1991) and access to food
301 resources after hatching (Cushing, 1982). We included the mean MLD from January to April,
302 during which time eggs and larvae are believed to aggregate at the base of the mixed layer
303 (Ahlstrom, 1959; Bailey, 1982).

304 The distribution of Pacific hake may be related to poleward flow in the California
305 Undercurrent (CU), with changes in flow aiding or impeding the poleward migration of adults
306 (Agostini et al., 2006, 2008; Benson et al., 2002; Dorn, 1995; Smith et al., 1990; Woodbury et
307 al., 1995). While Pacific hake spawn primarily over the continental slope, Bailey (1981)
308 suggested that the location of spawning is related to the CU, which usually occurs over the
309 continental slope at depths of 200 – 400 m. Flow in the undercurrent peaks during the spawning
310 period (Agostini, 2005), thus we included a metric of transport in the poleward undercurrent
311 (PU) from January to June to determine whether the transport of eggs and larvae might be
312 affected by changes in this feature (Tables 1 and A1).

313

314 **2.2.1.3 | Upwelling**

315 Wind-driven upwelling in the CCE drives its high biological productivity, supplying
316 nutrient-rich water to the surface layer and fueling the growth of phytoplankton that form the
317 base of the marine food web. To examine the impact of upwelling on recruitment, we used two
318 upwelling indices developed for the U.S. west coast: the Coastal Upwelling Transport Index
319 (CUTI) and the Biologically Effective Upwelling Transport Index (BEUTI) (Jacox et al. 2018).
320 CUTI and BEUTI provide estimates of the total volume of water and the total quantity of nitrate
321 upwelled or downwelled in a given time period, respectively. While CUTI is a measure of
322 physical upwelling transport, BEUTI is a measure of both the intensity of upwelling and the
323 quality of upwelled waters in terms of their nutrient content, which can strongly influence
324 productivity, independent of the surface wind strength (Jacox et al., 2016).

325 The input of nutrients and the timing of the spring transition from downwelling-favorable
326 to upwelling-favorable winds each year is critical to phytoplankton productivity, especially in the
327 northern CCE (Bograd et al., 2009). In addition to the two upwelling indices described above, we
328 included the timing of the spring transition as a predictor of hake recruitment due to its link to
329 hake production (Hollowed et al., 2009). The Julian day of the Mean Spring Transition Date
330 (SPTR), calculated using the Columbia Basin Research (CBR) Mean Method (Van Holmes,
331 2007), was used in our analysis. Briefly, the CBR Mean method averages daily upwelling
332 deviations from mean offshore transport at three sites along the Oregon and Washington coasts
333 (see Tables 1 and A1). The smoothed cumulative upwelling deviation indices are then examined
334 for spring minima, with the Julian day of this extreme listed as the CBR Mean Spring Transition
335 Date (Van Holmes, 2007).

336

337 **2.2.1.4 | Eddy kinetic energy**

338 Coastal eddies are mesoscale features that can retain early life stages and may contribute
339 to enhanced recruitment in marine fishes (Hare & Cowen, 1996; Owen, 1980; Sakuma &
340 Ralston, 1997; Sanchez & Gil, 2000; Vastano et al., 1992). Eddy kinetic energy (EKE) provides
341 a proxy for the intensity of mesoscale turbulence, which includes not only mesoscale eddies, but
342 also features such as meanders and fronts that can concentrate prey and lead to improved feeding
343 conditions. We included EKE as a predictor to investigate the effect of mesoscale variability on
344 Pacific hake recruitment during the post-spawning (January – April) and summer feeding (May –
345 September) periods from 31° – 34.5°N, 34.5 – 42.5°N, and 42.5° – 47°N.

346

347 **2.2.1.5 | Sea-surface height**

348 The collective expression of basin-scale processes (see Section 2.2.5 below) can result in
349 local changes in SSH. Thus, indices of SSH were included in our analysis to aid in testing the
350 consistency of mechanisms hypothesized to impact Pacific hake recruitment. Indices were
351 derived for the post-spawning (January – April) and summer feeding (May – September) periods
352 from the female preconditioning to the age-0 pelagic juvenile stage between 31° – 34.5°N, 34.5°
353 – 42.5°N, and 42.5° – 47°N.

354

355 **2.2.2 | Prey availability**

356 Prey availability in the months prior to spawning (here April – September) may affect
357 female condition, which, in turn, may affect the quality or number of eggs produced, or the
358 probability of spawning in a given year. We included recruitment of age-2 Pacific herring
359 (*Clupea pallasii*, $PREY_{pre,her}$) off the west coast of Vancouver Island (WCVI), representing
360 summer feeding conditions in Canadian waters, and log-transformed biomass of age-0 and age-1
361 juvenile hake ($\log PRED_{pre,juvhake}$), representing cannibalism by adults, from their most recent

362 stock assessments (Cleary et al., 2020; Grandin et al., 2020), as indices of prey abundance for the
363 female preconditioning period. Although euphausiids are a main prey item for Pacific hake
364 adults (Livingston & Bailey, 1985), there is no continuous time series available that represents
365 euphausiid abundance on their summer feeding grounds for the years examined in our analysis.
366 Thus, the link between hake recruitment and euphausiid abundance for this stage was not
367 explored.

368 Starvation during the early life stages is thought to be an important regulator of
369 recruitment in marine fishes, particularly at the time of first-feeding ('Critical Period' hypothesis,
370 Hjort, 1914, 1926) and during the period of drift from spawning grounds to juvenile nursery
371 areas, where the timing and abundance of food are important to survival ('Match-mismatch'
372 hypothesis, Cushing, 1972). In years with near-average ocean conditions, the diet of early-
373 juvenile Pacific hake transitions from copepods to euphausiids (Livingston & Bailey, 1985). We
374 developed indices of copepod abundance ($n\ m^{-2}$) as prey for the early and late larval stages
375 ($PREY_{larv.zp}$, $PREY_{latelarv.zp}$), and euphausiid abundance ($n\ m^{-2}$) as prey for the late larval and
376 juvenile stages ($PREY_{latelarv.eup}$, $PREY_{age0.eup}$) from surveys conducted by the California
377 Cooperative Oceanic Fisheries Investigations (CalCOFI) off the coast of southern California.
378 Weighted averages of copepod and euphausiid abundances from February to May were
379 calculated for each year. Copepod data were obtained from the Zooplankton Database
380 (<https://oceaninformatics.ucsd.edu/zoodb/secure/login.php>) and included pooled and unpooled
381 samples of Copepoda (all genera and species, all phases and stages) from night tows conducted
382 from February – May at lines 80 to 93 (Southern California). Euphausiid data were obtained
383 from the Brinton and Townsend Euphausiid Database

384 (<https://oceaninformatics.ucsd.edu/euphausiid/secure/login.php>) and included all genera and
385 species, all phases and stages collected from Feb – May from lines 77 to 93 (Southern
386 California).

387

388 **2.2.3 | Predation on recruits**

389 Size-specific predation is a major source of mortality for the early life stages of marine
390 fishes (Bailey & Houde, 1989; Houde, 2008). We included several indices of predator abundance
391 to examine the effects of predation on recruitment. Pacific hake have been shown to be important
392 prey of California sea lions (*Zalophus californianus*), for example. In the late 1970s they were
393 the most abundant prey in the diet of sea lions from San Miguel Island, off southern California,
394 with almost 49% of scats examined containing Pacific hake, mostly 1-2 year old fish (Antonelis
395 et al., 1984; Livingston & Bailey, 1985). Scat samples collected seasonally on San Clemente and
396 San Nicolas islands in the Southern California Bight from 1981 – 2015 also show evidence of
397 sea lion predation on age-0 and age-1 Pacific hake (< 30 cm in length) (A. Curtis, NOAA,
398 personal communication). We used estimated pup abundances from Laake et al. (2018) as an
399 estimate of California sea lion predation on Pacific hake ($PRED_{age0,cs1}$). Pup counts were used, as
400 they directly relate to predation on Pacific hake by females foraging around San Clemente and
401 San Nicolas islands (A. Curtis, NOAA, personal communication) by integrating both population
402 size and energetic demands of the population.

403 Arrowtooth flounder (*Atheresthes stomias*) is a highly piscivorous flatfish known to prey
404 on Pacific hake juveniles and adults (Buckley et al., 1999; Ressler et al., 2007; Sampson et al.,
405 2017). Pacific hake are the primary prey of arrowtooth flounder off Oregon and Washington
406 (Buckley et al., 1999). Although arrowtooth flounder are mostly found north of central California

407 (Best 1963), recent stomach content analysis work has found that young-of-the-year (YOY) fish
408 are consumed as well where their distributions overlap (Draper, 2022). We included an index of
409 arrowtooth flounder biomass from the most recent stock assessment (Sampson et al., 2017) as a
410 predator of age-0 Pacific hake ($PRED_{age0.atf}$).

411 Studies have shown evidence of cannibalism by age-1 fish on YOY Pacific hake (Smith
412 1995; Buckley & Livingston, 1997). Thus, we included log-transformed age-1 biomass of Pacific
413 hake from the 2020 stock assessment (Grandin et al., 2020) as an index of predation on age-0
414 juveniles ($\log PRED_{age0.age1hake}$).

415

416 **2.2.4 | Storm and calm periods**

417 Wind-induced mixing can affect the vertical distribution of plankton in the upper water
418 column, which, in turn, can influence feeding success and growth of larval fishes. Periods of
419 calm are associated with vertical stratification of the water column, aggregating prey in sufficient
420 concentrations to support successful foraging, growth, survival, and recruitment, while storm
421 events can disperse both larvae and food patches, leading to lower foraging success ('Stable
422 Ocean' hypothesis, Lasker, 1978, 1981). We included indices for the mean number of
423 ($CALM_{larv}$, $STORM_{larv}$), duration of ($CALMD_{larv}$, $STORMD_{larv}$), and time between
424 ($CALMB_{larv}$, $STORMB_{larv}$) distinct calm periods and storms events from February to May using
425 the methodology outlined in Turley & Rykaczewski (2019). Wind events were identified using
426 modeled wind output available from the NOAA National Centers for Environmental Prediction
427 Climate Forecast System Reanalysis model (Saha et al., 2010) for the region between 28° and
428 36°N. Storm periods were identified as intervals when the wind speeds were equal to or greater
429 than 10 m s^{-1} for a minimum of 18 h (and below this threshold for the preceding 96 h). A calm

430 period was identified when the wind speed was below 10 m s^{-1} for a minimum of 10 days and
431 wind speeds were above the same threshold during the preceding 18 h. A minimum of 10 days
432 was used because Pacific hake yolk-sac larvae must find food within this period, or irreversible
433 starvation occurs (Bailey, 1982). Further methodological details can be found in Turley &
434 Rykaczewski (2019).

435

436 **2.2.5 | Basin-scale processes**

437 *Bifurcation Index*

438 The NPC bifurcates into the poleward Alaska Current and the equatorward California
439 Current in a transition zone that ranges from about $42^\circ - 52^\circ \text{ N}$ (Freeland, 2006; Cummins and
440 Freeland, 2007). Variability in the north-south location of this bifurcation has been linked to
441 biological productivity in the CCE (Malick et al., 2017; Sydeman et al., 2011). We used an index
442 of the location of the NPC bifurcation (BI, Malick et al., 2017) to examine whether Pacific hake
443 recruitment was influenced by the positioning of the NPC, with the expectation that a northward-
444 shifted NPC would lead to higher productivity in the CCE and higher recruitment.

445

446 *El Niño-Southern Oscillation*

447 Variability in Pacific hake year-class strength has been linked to conditions related to
448 ENSO (Hollowed et al., 2001), which can cause warming of the upper ocean, depression of the
449 thermocline, weakening of upwelling intensity, and intensification of the CU (Chelton & Davis,
450 1982; Hickey, 1998; Hollowed, 1992; Jacox et al., 2015). We used the Oceanic Niño Index
451 (ONI), defined as the 3-month running average of sea surface temperature anomalies in the Niño
452 3.4 region ($5^\circ \text{S} - 5^\circ \text{N}$, $120^\circ - 170^\circ \text{W}$) (Trenberth, 1997), to index variability associated with El

453 Niño and La Niña events from the female preconditioning period (ONI_{pre}), through the larval
454 stages (ONI_{JA}), to summer feeding of age-0 pelagic juveniles ($ONIAS$).

455

456 *Pacific Decadal Oscillation*

457 The Pacific Decadal Oscillation (PDO), defined as the leading principle component of
458 monthly SST anomalies in the North Pacific poleward of 20°N (Mantua et al., 1997). The PDO
459 been shown to be correlated with indices of salmon survival in the Northeast Pacific (Burke et
460 al., 2013; Malick et al., 2009; Mantua et al., 1997) and the driver of inverse production regimes
461 between Alaska and west coast salmon stocks (Hare et al., 1999). The PDO was included as a
462 covariate for the female preconditioning period (PDO_{pre}), through the larval stages (PDO_{JA}), to
463 summer feeding of age-0 pelagic juveniles (PDO_{AS}).

464

465 *North Pacific Gyre Oscillation*

466 The North Pacific Gyre Oscillation (NPGO) measures changes in the circulation of the
467 North Pacific gyre and has been correlated with salinity, nutrient, and chlorophyll-a fluctuations
468 measured in long-term observations in the California Current and Gulf of Alaska (Di Lorenzo et
469 al., 2008). The NPGO has been linked to west coast salmon productivity (Malick et al., 2015,
470 2017) and may be important to the recruitment of Pacific hake. We included the NPGO as a
471 covariate in our analysis across all stages in our conceptual life history model (preconditioning
472 period, April – September; spawning to early larvae, January – April; late larvae to age-0
473 juveniles, April – September).

474

475 **2.3 | Recruitment residuals**

476 Model estimates of Pacific hake recruitment were taken from the most recent stock
477 assessment (here, Figure 3d, Figure 28 in Grandin et al., 2020). Specifically, we used the model-
478 estimated log deviations as the response variable, where the deviations were the annual
479 deviations from log median recruitment. Median recruitment was a function of the assumed
480 Beverton–Holt stock–recruitment relationship, aging error assumptions, and the data included in
481 the stock assessment model including the sampled age structure.

482 Our analysis covers recruitment residuals from 1981 – 2010, as the 1980 recruitment
483 deviation depends on the preconditioning period in 1979, which was not available in the CCE
484 ROMS output.

485

486 **2.4 | Model development**

487 Initial explorations of candidate variables led to a de facto reduction in the number of
488 models evaluated. Specifically, correlations among predictor variables and individual linear and
489 quadratic regressions for each predictor against recruitment deviations were calculated and
490 evaluated prior to model fitting and selection. Predictors that were strongly correlated (Figure
491 A2, $|r| > 0.70$) were not permitted in the same model (Dormann et al., 2013). Quadratic terms
492 were included in the main modeling exercise for individual hypothesized covariates where the
493 quadratic model fit better than the linear model (Akaike’s Information Criterion, AIC (Akaike,
494 1998), was < 2.0 that of the linear model). Based on preliminary model explorations, the
495 following covariates were included as potential quadratic predictors during model selection:
496 BEUTI ($UW_{pre.beu}$) from $41.5^\circ - 47.5^\circ N$ during the adult female preconditioning stage, and
497 cross-shore transport during the first-feeding (CST_{larv}) and late larval stages ($CST_{latelarv}$).

498 Due to the large number of hypotheses generated about the drivers of Pacific hake
499 recruitment, we used a three-step approach to model selection. First, a series of generalized
500 linear models (GLMs) were fitted for each of the seven stages in our Pacific hake conceptual life
501 history model, including all permutations of the ROMS covariates from our hypotheses and
502 excluding highly correlated terms (Figure A2, $|r| > 0.70$) from the same model. To prevent
503 overfitting, the number of ROMS predictors in a candidate model was limited to five (one
504 covariate per six data points in the time series). Predictors that were identified as potentially
505 quadratic were included in the models as a linear function and a quadratic function. The best-fit
506 models with $\Delta AICc < 2.0$ were retained for further consideration (Burnham & Anderson, 1998).
507 Second, generalized linear models (GLMs) were fit to all life stages combined and run with
508 ROMS predictor variables from the best-fit model for each stage, along with those variables
509 occurring in at least 3 of the stage-specific models with $\Delta AICc < 2.0$. Third, we retained all
510 ROMS variables appearing in models with $\Delta AICc < 2.0$ from the previous step, added the
511 predator, prey, and climate predictor variables, and re-evaluated the model selection for all life
512 stages combined. In total, 117,439 models were considered.

513 All analyses were conducted using R statistical software version 3.6.1 (R Core Team,
514 2020) using the Multi-model inference package (MuMIn, Barton, 2020) for model selection. Due
515 to a limit on the number of predictors allowed in the model fitting process (31), some covariates
516 were not included in the final step of model fitting. Terms that were highly correlated with
517 retained covariates (Figure A2, $PREY_{pre}$ with $PRED_{age0.age1hake}$ ($r = 0.88$); $CALMB_{larv}$ ($r = 0.76$)
518 and $CALMD_{larv}$ ($r = 0.81$) with $CALM_{larv}$) or were correlated with a similar covariate ($NPGO_{JA}$
519 with both $NPGO_{pre}$ ($r = 0.73$) and $NPGO_{AS}$ ($r = 0.92$); ONI_{JA} with ONI_{pre} ($r = 0.76$)), were
520 removed, although their hypothesized effects on recruitment were generally captured in the

521 analysis.

522

523 **2.5 | Model validation and testing**

524 The performance of the best-fit model for all stages in our conceptual life history model
525 was evaluated using (1) resampling with replacement of recruitment deviations to estimate R^2
526 values using 100 randomized data sets; (2) bootstrapping whole years with replacement to
527 estimate bias and calculate SE of the parameter estimates; (3) annual jackknife resampling to
528 determine the effect of any single year on the R^2 ; (4) resampling annual recruitment deviations
529 from a log-normal distribution using the annual mean and SD estimated from the assessment,
530 then recalculating recruitment residuals, and refitting the model 1,000 times; (5) refitting the
531 model using data for 1981 – 2005 and predicting recruitments deviations for 2006 – 2010; (6)
532 jackknife resampling to re-run the entire model-fitting and comparison exercise, to determine
533 whether removal of any individual year would change the selected predictor variables; and (7)
534 re-running the entire model fitting exercise 100 times using the re-sampled Pacific hake
535 recruitment deviations with error (from Step 4 above), comparing AICc-selected models from
536 each run. Finally, we used (8) jackknife resampling but fit only the years 1981 – 2005, compared
537 the resulting models to the best-fit model above, and used the 1981 – 2005 model to predict
538 recruitment deviations for 2006 – 2010.

539

540 **3 | RESULTS**

541 Model fitting identified a clear best-fit model for each stage in our conceptual life history
542 model for Pacific hake, with intercept-only models for the spawning, egg, and age-0 pelagic
543 juvenile stages (Table A2). The best-fit model for the adult female preconditioning stage, based

544 on the lowest AICc, included May – September eddy kinetic energy between 34.5° and 42.5°N
545 ($EKE_{pre.MS.c}$) and upwelling strength ($UW_{pre.cu}$), which together explained 31% of the
546 recruitment variability in Pacific hake. Alongshore transport (AST_{yolk}) and transport in the
547 poleward undercurrent (PU_{yolk}) during the yolk-sac stage explained 18% of the variability in
548 recruitment (Table A2). Cross-shelf transport north of Point Conception ($CST_{larv.n}$), along with
549 linear and quadratic predictors for cross-shelf transport south of Point Conception ($CST_{larv.s}$)
550 accounted for 16% of the recruitment variability for the first-feeding larval stage. Similarly,
551 linear and quadratic predictors for cross-shelf transport south of Point Conception during the late
552 larval stage ($CST_{latelarv.s}$) accounted for 22% of the variability in hake recruitment (Table A2).

553 All terms identified in the stage-specific best-fit models, along with those terms
554 appearing in three or more models with $\Delta AICc < 2.0$ (Table A3), were included in the next stage
555 of model fitting, where all life history stages were combined. Model fitting produced seven
556 candidate models with $\Delta AICc < 2.0$, which explained between 31% and 43% of the variability in
557 hake recruitment not accounted for by the stock-recruitment relationship in the assessment.
558 (Table A2). For the adult preconditioning stage, May – September EKE between 34.5° and
559 42.5°N ($EKE_{pre.MS.c}$) appeared in all seven models, while six models included upwelling strength
560 between 41.5° and 47.5°N ($UW_{pre.cu}$). Three models included alongshore transport during the
561 yolk-sac larval stage (AST_{yolk}) and two models included May – September EKE between 34.5°
562 and 42.5°N ($EKE_{MS.c}$). Linear and quadratic predictors for cross-shelf transport south of Point
563 Conception during the first-feeding larval stage ($CST_{larv.s}$, $CST^2_{larv.s}$) and the late larval stage
564 ($CST_{latelarv.s}$, $CST^2_{latelarv.s}$) each appeared in one model (Table A2). All terms appearing in the
565 seven models with $\Delta AICc < 2.0$ were carried over to the next step of model fitting.

566 The final step of model fitting, which combined the ROMS predictors identified in the

567 previous step with predator, prey, and climate predictors for all stages in our conceptual life
568 history model, identified five candidate models with a $\Delta AICc < 2.0$ (Table 2). The model with
569 the lowest AIC included five covariates (Figures 3, A1 and A3, Table 2), which explained 59%
570 of the variation in recruitment residuals from 1981 to 2010. Model predictions closely followed
571 the estimated recruitments from the stock assessment in 23 out of 30 years, with the exceptions
572 of 1984, 1989, 1990, 2000, 2005, 2007, and 2009 (Figure 4a). Recruitment deviations were
573 negatively correlated with the NPC Bifurcation Index (BI_{pre}), May – September EKE between
574 34.5° and $42.5^\circ N$ ($EKE_{pre.MS.c}$), and Pacific herring biomass off the WCVI ($PREY_{pre.her}$) during
575 the female spawner preconditioning stage (Figure 5). Negative correlations were also found with
576 northward alongshore transport between 50 – 100 m during the yolk-sac larval stage (AST_{yolk})
577 and the number of days between storm events during the first-feeding larval stage ($STORMB_{larv}$)
578 (Figure 5, Table 3). Standardized coefficients suggested that $EKE_{pre.MS.c}$ and BI_{pre} had the
579 strongest effect on recruitment, while the other predictors had relatively similar impacts (Table
580 3). All five $\Delta AICc < 2.0$ models included the $EKE_{pre.MS.c}$ predictor. The remaining four models
581 included combinations of the predictors described above, with additional terms including
582 predation on age-0 pelagic juveniles by age-1 hake ($PRED_{age.0age1.hake}$), upwelling strength during
583 the preconditioning stage ($UW_{pre.cu}$), which replaced the BI_{pre} predictor, and the number of calm
584 periods during the first-feeding larval stage ($CALM_{larv}$) (Tables 2 and A2).

585 There was weak correlation among the covariates in the best-fit model (Table 4).
586 Generalized variance inflation factor values (VIF), which measure how much the variance of the
587 estimated regression coefficients is inflated as compared to when the predictor variables are not
588 linearly related, were low (i.e., less than 2; Table 4). The diagnostics for the best-fit model show
589 good model fit (Figure 5) with residuals that did not show signs of autocorrelation (Figure A1).

590

591 **3.1 | Model testing and validation: best-fit model**

592 Randomly resampling the recruitment deviations (bootstrap with replacement) and re-
593 running the AIC-best model resulted in a median expected $R^2 = 0.16$ (95% C.I. = 0.03–0.41),
594 suggesting that the observed value of $R^2 = 0.59$ was not likely to be observed at random.

595 After removing individual years and refitting the best-fit model (jackknifing), there was
596 little impact on the model fit (Figures 4 and 5, median $R^2 = 0.59$ (95% C.I. = 0.55 – 0.67)).
597 Predicting the missing year from any iteration produced estimates very similar to those for the
598 full model (Figure 4a). The years that showed the highest impact on the model's ability to explain
599 the data were 1990 (increased to $R^2 = 0.70$) and 2002 (decreased to $R^2 = 0.54$, Figure 6).

600 Resampling annual recruitment deviations with error produced a slight decline in model
601 performance (median $R^2 = 0.56$ (95% C.I. = 0.50 – 0.62)). This suggests that uncertainty in the
602 time series of recruitment deviations (given the current stock assessment parameters) results in a
603 somewhat lower ability to explain the variability in recruitment.

604 When the entire model-fitting process was re-run using the jackknife resampling, the
605 results were fairly consistent with the primary analysis (Table 5). May – September EKE
606 between 34.5° and 42.5°N, the NPC Bifurcation Index, and Pacific herring biomass during the
607 adult female preconditioning stage appeared in 95%, 55%, and 11% of the models, respectively.
608 Alongshore transport during the yolk-sac larval stage and the number of days between storm
609 events appeared in 40% and 21% of the models, respectively. Other predictors of note were
610 upwelling strength between 41.5° and 47.5°N during the adult female preconditioning stage and
611 the number of calm periods during the first-feeding larval stage, which appeared in 40% and
612 37% of the models, respectively.

613 Resampling the recruitment deviations (with error) and re-running the entire model-
614 fitting exercise 100 times was mostly consistent with the AIC-best model from the primary
615 analysis (Table 6). Three of the five predictors from the AIC-best model were the most
616 commonly occurring predictors in the best-fit models from each iteration: $EKE_{pre.MS.c}$ (81% of
617 models), BI_{pre} (46%), AST_{yolk} (41%). Additional predictors included $CALM_{larv}$ (44%) and
618 $UW_{pre.cu}$ (40%). Other terms from the AIC-best model, $PREY_{pre.her}$ and $STORMB_{larv}$ occurred in
619 17% and 15% of the models, respectively.

620 Finally, jackknife resampling and re-running the entire model-fitting process for the 1981
621 – 2005 data supported the inclusion of only one term from the AIC-best model from the primary
622 analysis. The predictor for the NPC Bifurcation Index during the preconditioning stage (BI_{pre})
623 appeared in 55% of the best-fit models given the exclusion of a given year (Table 7). Predictors
624 representing predation on the early juvenile stages were important, with predation on age-0 fish
625 by age-1 hake ($\log PRED_{age0.age1.hake}$) and arrowtooth flounder predation on age-0 pelagic
626 juveniles appearing in 98% and 33% of the best-fit models from 1981 – 2005, respectively. The
627 linear and quadratic predictors for cross-shelf transport south of Point Conception during the
628 first-feeding larval stage ($CST_{larv.s}$, $CST^2_{larv.s}$) appeared in 76% and 71% of models, respectively
629 (Table 7). Other important predictors were the Ocean Niño Index during the adult female
630 preconditioning stage (ONI_{pre}) and the number of calm periods during the first-feeding larval
631 stage ($CALM_{larv}$), which appeared in 62% of and 24% the models, respectively. Surprisingly, the
632 $EKE_{pre.MS.c}$ predictor, which was a strong predictor in the both the jackknife and resampling
633 recruitment analyses, only appeared in 7% of the models, while $PREY_{pre.her}$ dropped to 2%.
634 However, jackknife resampling using the AIC-best model from the primary analysis did a good
635 job of predicting recruitment deviations for 1981 – 2005 ($R^2 = 0.63$, Figure 3b), although the

636 high recruitment events in 1990 and 2005 were underpredicted and recruitment in 1989 was
637 overpredicted. Our five-term model predicted recruitment deviations well when used to forecast
638 2006 – 2010, although it overpredicted recruitment in 2006 and underpredicted recruitment in
639 2009 and 2010 (Figure 3b). The AIC-best model from the jackknife resampling (BI_{pre} , ONI_{pre} ,
640 $CST_{larv.s}$, $CST^2_{larv.s}$, and $logPRED_{age0.age1.hake}$) did a very good job of predicting recruitment
641 deviations for 1981 – 2005 ($R^2 = 0.83$), yet only a marginal job for 1981 – 2010 ($R^2 = 0.44$).
642 Thus, the five-term Model 1 from the primary analysis appears to be an effective predictor of
643 Pacific hake recruitment variability.

644

645 **4 | DISCUSSION**

646 Our analyses revealed several potential drivers of recruitment variability in Pacific hake.
647 The five variables in the AIC-best model explained 59% of the variability in Pacific hake
648 recruitment not accounted for by estimates based exclusively on the spawning stock size.
649 Recruitment deviations were negatively correlated with May – September eddy kinetic energy
650 between 34.5° and 42.5°N, the location of the North Pacific Current bifurcation, and Pacific
651 herring biomass during the female spawner preconditioning stage, northward alongshore
652 transport during the yolk-sac larval stage, and the number of days between storm events during
653 the first-feeding larval stage. Upwelling strength during the preconditioning stage, the number of
654 calm periods during the first-feeding larval stage, and predation on age-0 pelagic juveniles by
655 age-1 hake were also important predictors that were negatively correlated with recruitment
656 (Table 2, A2). These findings suggest that multiple mechanisms likely affect Pacific hake
657 recruitment at different stages in their early life history (Figure 7). Intercept-only models for the
658 spawning, egg, and age-0 pelagic juvenile stages suggest that the hypotheses we evaluated for

659 these stages were not well explained by the ROMS data (Figure A2).

660 Eddy kinetic energy between May and September from Point Conception to Cape Blanco
661 during the female spawner preconditioning stage was the strongest driver of recruitment we
662 identified. Areas with higher mesoscale turbulence have energetic flow characterized by eddies,
663 meanders, and frontal structures, which are known to concentrate prey and improve feeding
664 opportunities for marine fishes (Logerwell & Smith, 2001; Bakun, 2006). As such, we expected
665 higher EKE to be associated with higher hake recruitment, yet the opposite relationship was
666 found. Decreasing recruitment with increasing EKE may be associated with its offshore
667 movement with the seasonal equatorward jet, which frequently separates from the coast at Cape
668 Blanco (Castelao et al., 2006; Strub & James, 2000). Fronts associated with upwelling filaments
669 may extend several hundred kilometers offshore (Castelao et al., 2006; Strub & James, 2000),
670 and while this could potentially benefit adult hake through expansion of their feeding habitat,
671 their movement offshore to less productive waters may result in poorer feeding conditions
672 overall, and greater energy expended on the return migration to their spawning grounds.
673 Similarly, Nieto et al. (2014) found that offshore transport had a negative effect on sardine
674 recruitment, despite the expansion of their spawning habitat farther offshore.

675 Previous studies have linked a northward-shifted NPC bifurcation to higher biomass and
676 productivity in the CCE, which likely results from the advective transport of nutrients and large-
677 bodied, lipid-rich zooplankton from the sub-arctic domain into the CCE, leading to enhanced
678 production in higher trophic level species (Malick et al., 2017; Sydeman et al., 2011). We
679 expected a similar response with hake. In contrast, we found that a southward-shifted NPC
680 bifurcation during the adult female preconditioning stage was linked to higher recruitment the
681 following year. High productivity in the northern CCE has been attributed to several

682 mechanisms, including a persistent nutrient supply through the dynamics of the Strait of Juan de
683 Fuca and the Columbia River, local upwelling enhancement by submarine canyons (e.g., Juan de
684 Fuca and Astoria canyons), and physical features that allow for the development and retention of
685 phytoplankton blooms on the shelf (Hickey & Banas, 2008). During the summer, the Columbia
686 River plume typically flows southwestward offshore of the Oregon shelf, while during the
687 winter, it flows northward over the Washington shelf (Hickey, 1989, 1998). The plume can
688 become bi-directional from summer to early fall, depending on the direction of prevailing winds
689 (Hickey et al., 2005). With a southward shifted NPC bifurcation (e.g., south of the Columbia
690 River), the northward flowing Alaska Current could impede the southwesterly flow of the
691 Columbia plume, advecting the highly productive waters off the coasts of Washington and
692 southern British Columbia northward, leading to better feeding conditions for adult hake on their
693 summer feeding grounds. In contrast, a northward-shifted NPC bifurcation (e.g., off the coast of
694 southern Vancouver Island) would likely result in poorer conditions for hake on their summer
695 feeding grounds, as the high productivity off the coasts of Washington and southern British
696 Columbia would instead be advected southward, with enhanced southwestward offshore flow of
697 plume waters.

698 Hake recruitment was negatively correlated with northward transport during the yolk-sac
699 larval stage (AST_{yolk} , January to April at 50 – 100 m), which was similar to the findings of
700 Schirripa & Colbert (2006), who linked higher sablefish recruitment with stronger southward
701 transport of surface waters (50 – 100 m) in February. Tolimieri et al. (2018) found that
702 northward transport of sablefish yolk-sac larvae at 1,000 – 1,200 m was associated with higher
703 recruitment, likely because it increased their overlap with northern zooplankton once they moved
704 to surface waters and started feeding. Increased southward transport could potentially increase

705 the overlap of first-feeding hake larvae with boreal copepods, which are larger, higher in fatty
706 acids, and provide a better food source than southern species (McFarlane & Beamish, 1992;
707 Peterson, 2009; Peterson & Keister, 2003). Reduced northward transport likely maintains yolk-
708 sac larvae in close proximity to their southern nursery grounds and may also improve survival by
709 reducing the spatial overlap of larval and early juvenile stages with age-1 hake, thereby reducing
710 cannibalism and competition for food resources (Buckley & Livingston, 1997; Smith, 1995).

711 We found that Pacific hake recruitment decreased as the number of days between storm
712 events increased during the first-feeding larval stage. This result was somewhat unexpected, as
713 calm periods in upwelling ecosystems are thought to facilitate vertical stratification of the water
714 column, aggregating fish larvae and prey at concentrations that support successful feeding,
715 survival, and recruitment (Lasker, 1978, 1981). For example, Peterman & Bradford (1987) found
716 that the mortality rate of northern anchovy larvae declined as the frequency of calm periods with
717 low wind speeds increased. However, Turley & Rykaczewski (2019) found that the number of
718 hake recruits per spawning stock biomass was negatively correlated to the number of distinct
719 calm periods per spawning season and that larval mortality significantly decreased as the number
720 of storm events increased. While storm-induced mixing can disrupt or dilute patches of plankton,
721 the authors suggested that these negative effects could be offset by increased contact rates
722 between first-feeding larvae and their prey (e.g., MacKenzie & Leggett, 1991; MacKenzie et al.,
723 1994). Turley & Rykaczewski (2019) also postulated that larval hake at the base of the mixed
724 layer could benefit from turbulence avoidance behavior by prey in the mixed layer, with prey
725 becoming more susceptible to predation as they swim downward (Franks, 2001). These
726 mechanisms could also explain the negative correlation found between recruitment and the
727 number of days between storm events in our study, as more frequent storm events would

728 maintain a downward flux of surface prey, leading to increased encounter rates, higher growth
729 and survival of first-feeding hake larvae, and higher recruitment. While increased turbulence
730 may initially improve feeding success by increasing encounter rates between predators and their
731 prey, this may only be up to a certain point, akin to the “Optimal Environmental Window”
732 hypothesis for upwelling (Cury & Roy, 1989). Research has shown that decreased ingestion rates
733 may occur at higher levels of turbulence through disruption of feeding patches, with decreased
734 reaction times of predators to increased prey velocities and decreased capture success also
735 impacting the ability of larvae to feed successfully (Landry et al., 1995 and references therein).
736 However, higher velocities of hake larvae and decreased capture success by their predators at
737 higher levels of turbulence may also help hake early life stages elude their predators, leading to
738 increased survival and higher recruitment.

739 Pacific herring biomass during the adult preconditioning stage was negatively correlated
740 with hake recruitment. This result was surprising, as we expected higher herring biomass to lead
741 to improved feeding conditions for adult hake, given that they become more piscivorous with age
742 and are a primary predator of herring off the west coast of Canada (Schweigert et al., 2010; Ware
743 and McFarlane, 1986, 1995). In a recent study, Godefroid et al. (2019) found that spatiotemporal
744 densities of Pacific herring and Pacific hake off the WCVI in summer were negatively
745 correlated, which the authors attributed to predation, although they noted this pattern might also
746 reflect different responses to environmental conditions or prey availability. The negative
747 relationship between hake recruitment and herring biomass during the adult preconditioning
748 stage in our study might result from competitive interactions between the two species.
749 Euphausiids are an important food source for Pacific hake across different life stages throughout
750 their range (Livingston & Bailey, 1985), accounting for 80 – 90 % of prey consumed, although

751 they decrease in importance for larger fish on their northward migration (Stauffer, 1985). Still,
752 higher herring biomass on the hake summer feeding grounds may reduce the abundance of
753 euphausiids, which could lead to poorer feeding conditions for adult hake, reduced condition
754 prior to spawning, and lower recruitment.

755 Our analysis identified additional covariates that were less consistently correlated with
756 recruitment, but may be influential in some years. In particular, hake recruitment was linked to
757 the NPGO, PDO, and upwelling during the adult female preconditioning stage, the number of
758 calm periods and duration of storm events during the first-feeding larval stage, euphausiid
759 abundance during the late larval stage, predation by age-1 hake during the age-0 pelagic juvenile
760 stage, and timing of the spring transition (Table 2). When a new model was fit with these
761 additional covariates outside of our main analysis, almost 63% of the variability in Pacific hake
762 recruitment deviations was explained, compared to 59% in the AIC-best model. However, model
763 diagnostics for these models were poor, indicating that they were likely overfitting the data.
764 Increased storm duration and the number of calm periods were likely linked with higher
765 recruitment due to the previously described mechanisms, with enhanced feeding as prey are more
766 frequently mixed downwards or descend to avoid turbulence during storms (Turley &
767 Rykaczewski, 2019). An alternative mechanism could be that increased turbulence associated
768 with increased storm duration would disrupt potential predation on larval hake as contacts rates
769 decreased with high turbulence (Landry et al., 1995 and references therein). Atmospheric forcing
770 associated with both the PDO and NPGO controls decadal modulation of the upwelling cells,
771 resulting in spatially varying responses of coastal upwelling, with a strong PDO signal north of
772 38°N and a strong NPGO signal south of 38°N (Di Lorenzo et al., 2008). Chhak & DiLorenzo
773 (2007) found differences in modeled depth of the upwelling cell between “warm” and “cool”

774 phases of the PDO, likely impacting nutrient flux and biological productivity, though differences
775 were not as strong in southern regions of the CCE compared to northern regions. Thus, the PDO
776 and NPGO may impact recruitment in Pacific hake through upwelling-related changes in
777 productivity and horizontal advection in the CCE.

778 While upwelling was not a predictor in our AIC-best model, it often appeared in other
779 candidate models (Tables 2 and A2). Upwelling fuels the CCE's high biological productivity and
780 as such, we expected that higher upwelling would be linked to higher hake recruitment. Instead,
781 we found that weaker upwelling north of 42°N from April to October during the adult female
782 preconditioning stage was linked to higher recruitment. Upwelling may impact feeding adults in
783 a number of ways. First, strong poleward flow is thought to aid Pacific hake adults in their
784 northward migration to their summer feeding grounds (Agostini et al., 2006; Benson et al., 2002;
785 Dorn, 1995; Smith et al., 1990). However, the spring transition to upwelling-favorable winds
786 coincides with the onset of predominantly equatorward flow and a reduced California
787 Undercurrent (Siedlecki et al., 2015). Thus, upwelling may impede the northward movement of
788 hake, increasing the energy expended swimming against strong southward currents during their
789 northward migration (Ressler et al., 2007), resulting in lower condition of pre-spawning females.
790 Second, upwelling may impact Pacific hake recruitment through bottom-up processes that affect
791 prey abundance and availability. Upwelling off Oregon and Washington is usually episodic, with
792 events lasting from days to weeks followed by periods of relaxation (Huyer et al., 1979; Huyer,
793 1983; Barth et al., 2000). The shoreward advection of near-surface waters during relaxation or
794 downwelling events has been shown to control larval recruitment (Farrell et al. 1991; Mackas et
795 al., 2001; Roughgarden et al., 1991; Shanks & Morgan, 2018), including that of euphausiids,
796 which are an important prey item for Pacific hake throughout their range (Livingston & Bailey,

797 1985). Indeed, high euphausiid recruitment has been linked to periods of downwelling or below-
798 average upwelling, which maintains larvae on the continental shelf instead of being transported
799 offshore into less productive oceanic waters (Mackas et al., 2001). High abundances of hake
800 have often been found in close proximity to high abundance patches of euphausiids near the
801 shelf-break, but the overlap has been less obvious farther offshore (Swartzman et al., 2001;
802 Phillips et al., 2022). Thus, while strong and persistent upwelling can transport phytoplankton
803 blooms and zooplankton prey far from shore via strong Ekman transport (Botsford et al., 2006;
804 Mackas et al., 2001), periods of reduced upwelling may be beneficial to Pacific hake adults on
805 their summer feeding grounds by increasing the abundance of their euphausiid prey via enhanced
806 recruitment, and also by maintaining spatial overlap with them through reducing their offshore
807 transport.

808 The multiple model validation methods applied to these data suggest that the AIC-best
809 model predictions were robust. Recruitment residuals fell well outside of the predicted 95%
810 confidence interval in 1990, 2007, and 2009 (Figure 4a). The latter years coincide with an
811 increase in the abundance and distribution of the Humboldt squid (*Dosidicus gigas*), which are
812 voracious predators that are known to prey on Pacific hake (Field et al., 2007; Litz et al., 2011).
813 Oddly, hake recruitment was high in 2009, when lower densities of juvenile hake were
814 coincident with the presence of Humboldt squid (Litz et al., 2011). However, higher hake
815 recruitment in 2009 could be linked to weaker than normal upwelling and extended relaxation
816 events in summer 2009 (Bjorkstedt et al., 2010), which may have maintained larvae and early
817 juveniles in close proximity to nearshore nursery habitats, providing better feeding conditions
818 compared to those found offshore. The lack of a clear link between the covariates examined in
819 our study and high recruitment in 1990 suggests that other variables not included here may be

820 important drivers of recruitment. The AIC-best model predictions from a leave-one-year-out
821 jackknife analysis provided predictions that fell within the 95% confidence limits of the fitted
822 AIC-best model in all years (Figure 4a). The AIC-best model predictions that used the available
823 data through 2005 and then predicted 2006 – 2010 resulted in similar predictions to those from
824 1981 – 2010 (Figure 4b). However, two of the recruitment predictors in the AIC-best model
825 ($PREY_{pre.her}$ and $STORMB_{larv}$) were no longer significant. This was likely due to higher values of
826 these predictors at the end of the time series, along with above average recruitment (except in
827 2007), which were removed when using the 1981 through 2005 training data set.

828 Predation on age-0 hake by the preceding cohort was an important predictor of hake
829 recruitment in our jackknife analysis. Previous studies have shown that year-class strength was
830 largely determined within the first few months of hatching (Bailey & Francis, 1985; Hollowed &
831 Bailey, 1989), but predation on juvenile hake was not considered to be a major source of
832 recruitment variability (Bailey & Francis, 1995). However, other studies have suggested that
833 recruitment may be affected by adjacent-cohort cannibalism (Buckley & Livingston, 1997;
834 Smith, 1995). Alternatively, increased competition for food may lead to reduced recruitment in a
835 cohort that follows a successful one (Buckley & Livingston, 1997; Smith, 1995).

836 Arrowtooth flounder biomass was also an important predictor during the model testing
837 and validation process. Pacific hake are the primary diet of arrowtooth flounder off the Oregon
838 and Washington coasts (Buckley et al., 1999). The positive relationship with recruitment could
839 potentially be explained by increased predation on older (age-2+) hake on their summer feeding
840 grounds when arrowtooth flounder biomass is high. Density-dependent mortality due to
841 cannibalism on age-0 and age-1 juvenile hake by older fishes is likely related to the amount of
842 spatial overlap between juvenile and adult fish (Buckley & Livingston, 1997). Thus, the higher

843 levels of recruitment seen when arrowtooth flounder biomass is high may reflect increased
844 predation on adult hake, which would reduce the amount of adult cannibalism on age-1 and YOY
845 fish (Buckley & Livingston, 1997). The arrowtooth flounder spawning biomass experienced a
846 period of fairly rapid decline during the 1970s and subsequent increase through the 1980s,
847 reaching a peak in 1991 (Sampson et al., 2017). Since then, spawning biomass has declined,
848 reaching a low in 2010 (Sampson et al., 2017), which may explain the lack of relationship
849 between recruitment and arrowtooth flounder predation in the 1981 – 2010 time series.

850 In comparison to recruitment drivers identified for other CCE species using the same
851 approach, the lack of a temperature predictor in any of the models for Pacific hake is notable.
852 Degree days during the female preconditioning period was found to be an important predictor of
853 both sablefish (Tolimieri et al., 2018) and petrale sole recruitment (Haltuch et al., 2020). Pacific
854 hake distribution is driven by interactions between age composition and temperature (Malick et
855 al., 2020). However, temperature has a non-linear effect on the distribution of immature hake
856 (i.e., age-2 fish) (Malick et al., 2020), and non-linearity could potentially explain the lack of a
857 relationship between temperature and recruitment in our GLMs. Reproduction and early
858 development in marine fishes are particularly sensitive to changes in temperature (Pepin, 1991;
859 Pörtner et al., 2001; Van Der Kraak & Pankhurst, 1997) and temperature can affect growth and
860 survival indirectly by altering the species composition, nutritional quality, and seasonal
861 distribution of prey (Asch, 2015; Keister et al., 2011; Fietcher et al., 2015; Peterson, 2009;
862 Peterson & Keister, 2003). Another potential explanation for the lack of relationship between
863 temperature and recruitment may be that adult hake seek out a particular temperature or narrow
864 range of temperatures and/or environmental conditions over which to spawn, though Agostini et
865 al. (2006) found that Pacific hake habitat was associated with subsurface poleward flow rather

866 than a specific temperature range. If spawning is initiated when specific water mass properties or
867 a particular temperature range is encountered, as suggested by Bailey et al. (1982), then a strong
868 temperature response in post-spawning stages would not be expected. In addition, because hake
869 spawn at depth where temperatures are cooler, their propagules are released into a relatively
870 stable thermal environment that experiences less year-to-year variability compared to surface
871 waters. Eggs and larvae are found in waters below the mixed layer, which are insulated to some
872 extent from temperature fluctuations in the surface mixed layer above (Bailey, 1982). This
873 relatively stable environment may explain why the early growth of hake larvae shows little
874 variation from season to season (Bailey, 1982; Butler & Nishimoto, 1997). Thus, Pacific hake
875 likely respond differently to climate variability compared to other species that occupy different
876 parts of the water column during their life histories.

877 Based on the results of the current study, it appears that cohort strength is established
878 between the larval and early juvenile stages, but conditions experienced by adult females prior to
879 spawning are also important. Previous research has shown that the survival of larval Pacific hake
880 is strongly influenced by the environmental conditions experienced during the first few months
881 after spawning (Agostini, 2005; Bailey, 1981; Bailey & Francis, 1985; Bailey et al., 1986;
882 Hollowed, 1992;), which suggests that year-class strength is set during the first year of life.
883 Increased recruitment has been linked to weak offshore transport in early winter (Bailey 1980,
884 1981; Bailey & Francis, 1985; Hollowed & Bailey, 1989), warm January sea surface temperature
885 (Bailey & Francis 1985; Hollowed & Bailey, 1989), and increased upwelling in March
886 (Hollowed & Bailey, 1989). However, we did not find significant relationships between
887 recruitment and covariates for temperature and upwelling during the early life stages, although
888 upwelling during the preconditioning stage was important in two of the models with a $\Delta AICc <$

889 2. One potential explanation for discrepancies between our analysis and past research findings
890 could be that earlier studies were limited by shorter time series (e.g., Bailey, 1981) and
891 previously observed relationships have not persisted over time. Indeed, associations between
892 environmental conditions and biological responses are often non-stationary in time (Myers,
893 1998). For example, regression models assuming stationary climate–salmon relationships were
894 found to be inappropriate over multidecadal time scales (1965 – 2012) in a recent study of
895 salmon (*Onchorynchus* spp.) productivity in the Gulf of Alaska (Litzow et al., 2018).
896 Relationships between recruitment, the prevalence of density dependence, and environmental
897 drivers have also been shown to differ between PDO regimes for bocaccio rockfish (*Sebastes*
898 *paucispinis*) (Tolimieri & Levin, 2005; Zabel et al., 2011). For Pacific hake, the changing
899 relationships between recruitment strength and temperature and upwelling during the 1970s
900 (Bailey, 1981) and the 1980s (Bailey & Francis, 1985) suggest that climate-recruitment
901 relationships may also be non-stationary. Another potential explanation for why our recruitment
902 predictors do not align with those found in previous studies is that different timeframes were
903 used to calculate the means for each predictor, obscuring conditions linked to high recruitment
904 events. For example, Hollowed & Bailey (1989) found that successful year-classes of Pacific
905 hake occurred after periods of low upwelling during early winter (either January or February)
906 followed by a period of intense upwelling in March. Our predictors for upwelling during the
907 yolk-sac and first-feeding larval stages were calculated over January – April and February –
908 May, respectively, thus, they likely would not capture specific upwelling events in March linked
909 to high recruitment.

910 One limitation of our study is that the CCE ROMS domain only covers the U.S. west
911 coast, thus we are unable to address oceanographic conditions in Canadian or Mexican waters

912 that might be important to Pacific hake recruitment. Several predictors did represent conditions
913 outside of the ROMS domain that could potentially affect hake recruitment. These included
914 basin-scale climate indices (e.g., ONI, PDO) and covariates representing the effects of storm
915 events and calm periods on first-feeding larvae off the coast of Baja California. Constraining the
916 spatial domain of the storm and calm covariates to that of the ROMS output ($31^{\circ} - 36^{\circ}\text{N}$ vs. 28°
917 $- 36^{\circ}\text{N}$) during exploratory analyses resulted in a change in model predictors, with predation on
918 age-0s by age-1 hake replacing the $\text{CALM}_{\text{larv}}$ predictor. This suggests that predation by the
919 preceding cohort may be an important driver of recruitment off southern California where
920 overlap between age-1 and YOY hake may be greater, while calm periods during the first-
921 feeding larval stage may be more important off Baja California. This finding underscores the fact
922 that environmental conditions outside of the ROMS region likely play an important role in hake
923 recruitment. Thus, regional ocean reanalyses with broader spatial coverage would be helpful to
924 include in future studies of recruitment drivers of species with distributions that cross
925 international boundaries.

926 Finally, while our analysis assumes that Pacific hake spawn off the coast of southern
927 California during the winter months, spawning has never been directly observed. Ressler et al.
928 (2007) suggest that the location of spawning is variable, with groups spawning in different
929 places, well north of where the classic model would suggest in some years (see their Figure 8).
930 Several studies have reported finding hake eggs and larvae in the northern region of the CCE in
931 some years (Auth et al., 2018; Brodeur et al., 2019; Hollowed, 1992; Phillips et al., 2007) and
932 future studies should consider alternative spawning grounds, as well as potential shifts in the
933 timing of spawning. Indeed, recent hake maturity work has shown that individuals may be
934 spawning outside of the traditional winter spawning season coast-wide (M. Head, NOAA,

935 personal communication).

936 Our work substantially updates the understanding of drivers of Pacific hake recruitment
937 in the CCE and has the potential to influence the stock assessment process, ecosystem
938 assessments, and management strategy evaluations (MSEs) (e.g., Hollowed et al., 2009). In the
939 current hake stock assessment, recruitment estimates in the current and previous years, and for 2-
940 3 year projections into the future are informed only by the stock-recruitment relationship and the
941 large standard deviation that is assumed for annual variability in recruitment. Empirical or
942 model-based information about the scale or direction of drivers of recruitment could reduce
943 uncertainty in recruitment in those years, which would reduce uncertainty in estimates of stock
944 status and allow the stock assessment scientists to provide more precise catch advice (Kaplan et
945 al., 2016; Siedlecki et al., 2016; Tommasi et al., 2017). Moreover, by annually updating
946 environmental predictors to inform recruitment forecasting based on both observed
947 oceanographic conditions and potentially sub-annual forecasts of environmental conditions
948 (Jacox et al., 2017; Siedlecki et al., 2016), managers and stakeholders could be provided with
949 leading environmental indicators of recruitment (Jacox et al., 2020). Recruitment indicators
950 could be used by stakeholders to reduce uncertainty in business planning, or more formally
951 within the management process by informing a risk assessment that could provide context for the
952 binational annual catch level negotiations (e.g., Dorn and Zador, 2020).

953 Our results can also inform assessments of hake's vulnerability to climate change and an
954 ongoing climate-informed MSE focused on hake. Several of the indicators of recruitment we
955 identified come from a ROMS product, and a related product has recently been forecasted to
956 2100 (Pozo Buil et al., 2021), meaning we can use forecasts of the drivers we identified to begin
957 to understand how recruitment variability could change under future ocean conditions.

958 Additionally, a management strategy evaluation for hake has shown that a northward distribution
959 shift in the population could result in diminished ability of the U.S. fishery to catch fish in U.S.
960 waters (Jacobsen et al., 2021). Our results identifying drivers of recruitment and the future
961 ROMS projections together can be used to develop scenarios of future recruitment, which when
962 combined with projecting movement, allow us to begin to understand the impacts of climate
963 change on multiple aspects of Pacific hake life history and the consequences for the management
964 of the binational fishery.

965

966 **ACKNOWLEDGEMENTS**

967 We thank Drs. Melissa Haltuch, Jim Hastie, Chris Harvey, and Michael Malick for discussion in
968 general and comments on the manuscript and Dr. Jacyln Cleary for providing the Pacific herring
969 data used in our analysis. Dr. Haltuch and Dr. Tolimieri co-developed the basis for the
970 methodological approach applied in this study. Reviews from Dr. Elizabeth Phillips and two
971 anonymous reviewers greatly improved this manuscript. ROMS model output was provided by
972 the UC Santa Cruz Ocean Modeling Group and is available at <http://oceanmodeling.ucsc.edu>.
973 Plankton sample analysis supported by NSF grants to M.D. Ohman, Scripps Institution of
974 Oceanography and by the SIO Pelagic Invertebrates Collection. Funding for C.D. Vestfals was
975 provided by the Northwest Fisheries Science Center and the California Current Integrated
976 Ecosystem Assessment Program through an agreement with the National Research Council.

977

978 **CONFLICT OF INTEREST**

979 The authors do not have any conflicts of interest, commercial or otherwise, that have influenced
980 the findings of this research.

981
982
983
984
985
986
987
988
989
990
991
992
993
994
995
996
997
998
999
1000
1001
1002
1003

AUTHOR CONTRIBUTIONS

K.N.M., N.T., M.E.H., I.G.T, and A.M.B conceived the study. C.D.V. developed the conceptual life history model. N.T. developed and C.D.V. undertook statistical analyses. M.G.J. provided the oceanographic expertise and ROMS model outputs for the study. B.D.T. provided expertise and code for the storm and calm indices used in this study. C.D.V. drafted the manuscript with input and revisions from all authors.

ORCID

- Cathleen D. Vestfals <https://orcid.org/0000-0002-9885-1430>
- Nick Tolimieri <https://orcid.org/0000-0003-0581-9915>
- Mary E. Hunsicker <https://orcid.org/0000-0002-3036-1515>
- Brendan D. Turley <https://orcid.org/0000-0001-7522-1885>

DATA AVAILABILITY STATEMENT

The data associated with this manuscript are available through the NOAA Northwest Fisheries Science Center, Fishery Resource Analysis and Monitoring Division. The code used for the analysis is available on GitHub (<https://github.com/pacific-hake/recruitment-index>). Outputs from the regional ocean reanalysis are available from the UC Santa Cruz ocean modeling group (oceanmodeling.ucsc.edu).

1004 **REFERENCES**

1005

1006 Agostini, V. N. (2005). Climate, ecology and productivity of Pacific sardine (*Sardinops sagax*)
1007 and hake (*Merluccius productus*). Doctoral dissertation, University of Washington,
1008 Seattle, WA.

1009

1010 Agostini, V. N., Francis, R. C., Hollowed, A. B., Pierce, S. D., Wilson, C., & Hendrix, A.
1011 N. (2006). The relationship between Pacific hake (*Merluccius productus*) distribution
1012 and poleward subsurface flow in the California Current System. *Canadian Journal of*
1013 *Fisheries and Aquatic Sciences*, 63(12), 2648-2659. <https://doi.org/10.1139/f06-139>
1014 © Canadian Science Publishing or its licensors.

1015

1016 Agostini, V. N., Hendrix, A. N., Hollowed, A. B., Wilson, C. D., Pierce, S. D., & Francis,
1017 R. C. (2008). Climate–ocean variability and Pacific hake: a geostatistical modeling
1018 approach. *Journal of marine systems*, 71(3-4), 237-248.
1019 <https://doi.org/10.1016/j.jmarsys.2007.01.010>

1020

1021 Ahlstrom, E. H. (1959). Vertical distribution of pelagic fish egg and larvae off California and
1022 Baja California. *Fishery Bulletin*, 60, 107-146.

1023

1024 Ahlstrom, E. H., & Counts, R. C. (1955). Eggs and larvae of the Pacific hake *Merluccius*
1025 *productus*. U.S. Government Printing Office.

1026

1027 Akaike, H. (1998). Information theory and an extension of the maximum likelihood principle. In:
1028 *Selected Papers of Hirotugu Akaike*. Springer, New York, NY

1029

1030 Antonelis, G. A., Fiscus, C. H., & DeLong, R. L. (1984). Spring and summer prey of
1031 California sea lions, *Zalophus californianus*, at San Miguel Island, California, 1978–
1032 79. *Fishery Bulletin*, 82(1), 67-75.

1033

1034 Asch, R. G. (2015). Climate change and decadal shifts in the phenology of larval fishes in
1035 the California Current ecosystem. *Proceedings of the National Academy of*
1036 *Sciences*, 112(30), E4065-E4074. <https://doi.org/10.1073/pnas.1421946112>

1037

1038 Auth, T. D., Daly, E. A., Brodeur, R. D., & Fisher, J. L. (2018). Phenological and distributional
1039 shifts in ichthyoplankton associated with recent warming in the northeast Pacific
1040 Ocean. *Global change biology*, 24(1), 259-272. <https://doi.org/10.1111/gcb.13872>

1041

1042 Bailey, K. M. (1980). Recent changes in the distribution of hake larvae: causes and
1043 consequences. *California Cooperative Oceanic Fisheries Investigations Report*, 21,
1044 167-171.

1045

1046 Bailey, K. M. (1981). Larval transport and recruitment of Pacific hake *Merluccius productus*.
1047 *Marine Ecology Progress Series*, 6(1), 1-9.
1048 <https://www.int-res.com/articles/meps/6/m006p001.pdf>

1049

- 1050 Bailey, K. M. (1982). The early life history of the Pacific hake, *Merluccius productus*. *Fishery*
1051 *Bulletin*, 80, 589-598.
1052
- 1053 Bailey, K. M., Francis, R. C., & Mais, K. F. (1986). Evaluating incidental catches of 0-age
1054 Pacific hake to forecast recruitment. *California Cooperative Oceanic Fisheries*
1055 *Investigations Report*, 27, 109-112.
1056
- 1057 Bailey, K. M., Francis, R. C., & Stevens, P. R. (1982). The life history and fishery of Pacific
1058 whiting, *Merluccius productus*. NWAFC Processed Report 82-03, 87 p.
1059
- 1060 Bailey, K.M. & Francis, R.C. (1985). Recruitment of Pacific Whiting, *Merluccius productus*, and
1061 the Ocean Environment. *Marine Fisheries Review*, 47(2), 8-15.
1062 <https://spo.nmfs.noaa.gov/sites/default/files/pdf-content/MFR/mfr472/mfr4723.pdf>
1063
- 1064 Bailey, K. M., & Houde, E. D. (1989). Predation on eggs and larvae of marine fishes and the
1065 recruitment problem. In: *Advances in Marine Biology* (Vol. 25, pp. 1-83). Academic
1066 Press. [https://doi.org/10.1016/S0065-2881\(08\)60187-X](https://doi.org/10.1016/S0065-2881(08)60187-X)
1067
- 1068 Bakun, A. (2006). Fronts and eddies as key structures in the habitat of marine fish larvae:
1069 opportunity, adaptive response and competitive advantage. *Scientia Marina*, 70(A2), 105-
1070 122. <https://doi.org/10.3989/scimar.2006.70s2105>
1071
- 1072 Barth, J. A., Pierce, S. D., & Smith, R. L. (2000). A separating coastal upwelling jet at Cape
1073 Blanco, Oregon and its connection to the California Current System. *Deep Sea Research*
1074 *Part II: Topical Studies in Oceanography*, 47(5-6), 783-810.
1075 [https://doi.org/10.1016/S0967-0645\(99\)00127-7](https://doi.org/10.1016/S0967-0645(99)00127-7)
1076
- 1077 Barton, K. (2020). MuMIn: multi-model inference. R package version 1.43.17.
1078
- 1079 Becker, E. A., Forney, K. A., Redfern, J. V., Barlow, J., Jacox, M. G., Roberts, J. J., &
1080 Palacios, D. M. (2019). Predicting cetacean abundance and distribution in a
1081 changing climate. *Diversity and Distributions*, 25(4), 626-643.
1082 <https://doi.org/10.1111/ddi.12867>
1083
- 1084 Benson, A. J., McFarlane, G. A., Allen, S. E., & Dower, J. F. (2002). Changes in Pacific hake
1085 (*Merluccius productus*) migration patterns and juvenile growth related to the 1989 regime
1086 shift. *Canadian Journal of Fisheries and Aquatic Sciences*, 59(12), 1969-1979.
1087 <https://doi.org/10.1139/f02-156>
1088
- 1089 Berger, A. M., Edwards, A. M., Grandin, C. J., & Johnson, K. F. (2019). Status of the Pacific
1090 Hake (whiting) stock in U.S. and Canadian waters in 2019. Prepared by the Joint
1091 Technical Committee of the U.S. and Canada Pacific Hake/Whiting Agreement, National
1092 Marine Fisheries Service and Fisheries and Oceans Canada. 249 p.
1093
- 1094 Best, E. A. (1963). Contribution to the biology of the Pacific hake, *Merluccius productus*
1095 (Ayres). *California Cooperative Oceanic Fisheries Investigations Report*, 9, 51-56.

1096
1097 Bjorkstedt, E. P., Goericke, R., McClatchie, S., Weber, E., Watson, W., Lo, N., ... &
1098 Munger, L. M. (2010). State of the California Current 2009-2010: Regional
1099 variation persists through transition from La Niña to El Niño (and back?). *California*
1100 *Cooperative Oceanic Fisheries Investigations Report*, 51, 39-69.
1101
1102 Burnham, K. P., & Anderson, D. R. (1998). Model selection and inference: A practical
1103 information-theoretic approach. New York, NY: Springer-Verlag.
1104
1105 Butler, J. L., & Nishimoto, R. N. (1997). Growth and cohort dynamics of larval Pacific hake
1106 (*Merluccius productus*). *California Cooperative Oceanic Fisheries Investigations Report*,
1107 38, 63-68.
1108
1109 Bograd, S. J., Schroeder, I., Sarkar, N., Qiu, X., Sydeman, W. J., & Schwing, F. B. (2009).
1110 Phenology of coastal upwelling in the California Current. *Geophysical Research Letters*,
1111 36(1). <https://doi.org/10.1029/2008GL035933>
1112
1113 Botsford, L. W., Lawrence, C. A., Dever, E. P., Hastings, A., & Largier, J. (2006). Effects of
1114 variable winds on biological productivity on continental shelves in coastal upwelling
1115 systems. *Deep Sea Research Part II: Topical Studies in Oceanography*, 53(25-26), 3116-
1116 3140. <https://doi.org/10.1016/j.dsr2.2006.07.011>
1117
1118 Brodeur, R. D., Auth, T. D., & Phillips, A. J. (2019). Major shifts in pelagic micronekton and
1119 macrozooplankton community structure in an upwelling ecosystem related to an
1120 unprecedented marine heatwave. *Frontiers in Marine Science*, 6, 212.
1121 <https://doi.org/10.3389/fmars.2019.00212>
1122
1123 Brodie, S., Jacox, M. G., Bograd, S. J., Welch, H., Dewar, H., Scales, K. L., ... & Lewison, R. L.
1124 (2018). Integrating dynamic subsurface habitat metrics into species distribution models.
1125 *Frontiers in Marine Science*, 5, 219. <https://doi.org/10.3389/fmars.2018.00219>
1126
1127 Buckley, T. W., & Livingston, P. A. (1997). Geographic variation in the diet of Pacific hake,
1128 with a note on cannibalism. *California Cooperative Oceanic Fisheries Investigations*
1129 *Report*, 38, 53-62.
1130
1131 Buckley, T. W., Tyler, G. E., Smith, D. M., & Livingston, P. A. (1999). Food habits of some
1132 commercially important groundfish off the coasts of California, Oregon, Washington, and
1133 British Columbia. *NOAA Technical Memorandum NMFS-AFSC*, 102, 173.
1134
1135 Burke, B. J., Peterson, W. T., Beckman, B. R., Morgan, C., Daly, E. A., & Litz, M. (2013).
1136 Multivariate models of adult Pacific salmon returns. *PloS ONE*, 8(1), e54134.
1137 <https://doi.org/10.1371/journal.pone.0054134>
1138
1139 Burnham, K. P., & Anderson, D. R. (1998). Practical use of the information-theoretic approach.
1140 In: *Model selection and inference* (pp. 75-117). Springer, New York, NY.
1141

- 1142 Cass-Calay, S. L. (1997). Relation of mean growth rate to concentration of prey-sized particles
1143 for larvae of Pacific hake (*Merluccius productus*). *California Cooperative Oceanic*
1144 *Fisheries Investigations Report*, 69-76.
1145
- 1146 Castelao, R. M., Mavor, T. P., Barth, J. A., & Breaker, L. C. (2006). Sea surface temperature
1147 fronts in the California Current System from geostationary satellite observations. *Journal*
1148 *of Geophysical Research: Oceans*, 111(C9). <https://doi.org/10.1029/2006JC003541>
1149
- 1150 Chelton, D. B., & Davis, R. E. (1982). Monthly mean sea-level variability along the west coast
1151 of North America. *Journal of Physical Oceanography*, 12(8), 757-784.
1152 [https://doi.org/10.1175/1520-0485\(1982\)012<0757:MMSLVA>2.0.CO;2](https://doi.org/10.1175/1520-0485(1982)012<0757:MMSLVA>2.0.CO;2)
1153
- 1154 Chereskin, T. K., & Trunnell, M. (1996). Correlation scales, objective mapping, and absolute
1155 geostrophic flow in the California Current. *Journal of Geophysical Research: Oceans*,
1156 101(C10), 22619-22629. <https://doi.org/10.1029/96JC02004>
1157
- 1158 Chezik, K. A., Lester, N. P., & Venturelli, P. A. (2014). Fish growth and degree-days I:
1159 selecting a base temperature for a within-population study. *Canadian Journal of*
1160 *Fisheries and Aquatic Sciences*, 71(1), 47-55. <https://doi.org/10.1139/cjfas-2013-0295>
1161
- 1162 Chhak, K., & Di Lorenzo, E. (2007). Decadal variations in the California Current upwelling
1163 cells. *Geophysical Research Letters*, 34(14).
1164
- 1165 Cleary, J., Hawkshaw, S., Grinnell, M., Grandin, C., Postlethwaite, V., Rusch, B., &
1166 Christensen, L. (2020). Stock status update with application of management procedures
1167 for Pacific herring (*Clupea pallasii*) in British Columbia: Status in 2020 and forecast for
1168 2021. Canadian Science Advisory Secretariat. Pacific Region. Science Response
1169 2021/001. <https://waves-vagues.dfo-mpo.gc.ca/Library/40966264.pdf>
1170
- 1171 Cooke, K. D., Holmes, J., Fleischer, G. W., Thomas, R. E., & Ressler, P. H. (2006).
1172 Distributional changes observed in the geographic range of Pacific hake (*Merluccius*
1173 *productus*) in association with ocean conditions off the Pacific coast of Canada and the
1174 United States. *ICES CM*, 2006, 01.
1175 <https://www.ices.dk/sites/pub/CM%20Documents/2006/B/B0106%20.pdf>
1176
- 1177 Cummins, P. F., & Freeland, H. J. (2007). Variability of the North Pacific Current and its
1178 bifurcation. *Progress in Oceanography*, 75(2), 253-265.
1179 <https://doi.org/10.1016/j.pocean.2007.08.006>
1180
- 1181 Cury, P., & Roy, C. (1989). Optimal environmental window and pelagic fish recruitment success
1182 in upwelling areas. *Canadian Journal of Fisheries and Aquatic Sciences*, 46(4), 670-
1183 680.
1184
- 1185 Cushing, D. H. (1972). The production cycle and the numbers of marine fish. In *Symposia of the*
1186 *Zoological Society of London*, 29, 213-232.
1187

1188 Cushing, D. H. (1982). *Climate and fisheries*. London, UK: Academic Press.
1189

1190 Di Lorenzo, E. (2003). Seasonal dynamics of the surface circulation in the Southern California
1191 Current System. *Deep Sea Research Part II: Topical Studies in Oceanography*, 50(14-
1192 16), 2371-2388. [https://doi.org/10.1016/S0967-0645\(03\)00125-5](https://doi.org/10.1016/S0967-0645(03)00125-5)
1193

1194 Di Lorenzo, E., Schneider, N., Cobb, K. M., Franks, P. J. S., Chhak, K., Miller, A. J., ... &
1195 Powell, T. M. (2008). North Pacific Gyre Oscillation links ocean climate and ecosystem
1196 change. *Geophysical Research Letters*, 35(8). <https://doi.org/10.1029/2007GL032838>
1197

1198 Dong, C., Idica, E. Y., & McWilliams, J. C. (2009). Circulation and multiple-scale variability in
1199 the Southern California Bight. *Progress in Oceanography*, 82(3), 168-190.
1200 <https://doi.org/10.1016/j.pocean.2009.07.005>
1201

1202 Dormann, C. F., Elith, J., Bacher, S., Buchmann, C., Carl, G., Carré, G., ... & Lautenbach, S.
1203 (2013). Collinearity: a review of methods to deal with it and a simulation study
1204 evaluating their performance. *Ecography*, 36(1), 27-46.
1205 <https://doi.org/10.1111/j.1600-0587.2012.07348.x>
1206

1207 Dorn, M. W. (1995). The effects of age composition and oceanographic conditions on the annual
1208 migration of Pacific whiting, *Merluccius productus*. *California Cooperative Oceanic*
1209 *Fisheries Investigations Report*, 36, 97-105.
1210

1211 Dorn, M.W. & Zador, S.G. (2020). A risk table to address concerns external to stock
1212 assessments when developing fisheries harvest recommendations. *Ecosystem Health and*
1213 *Sustainability*, 6(1), p.1813634. <https://doi.org/10.1080/20964129.2020.1813634>
1214

1215 Draper, D. L. (2022). Food habit variability of arrowtooth flounder (*Atheresthes stomias*) along
1216 the US west coast. *Fisheries Research*, 248, 106205.
1217 <https://doi.org/10.1016/j.fishres.2021.106205>
1218

1219 Farrell, T. M., Bracher, D., & Roughgarden, J. (1991). Cross-shelf transport causes recruitment
1220 to intertidal populations in central California. *Limnology and Oceanography*, 36(2), 279-
1221 288. <https://doi.org/10.4319/lo.1991.36.2.0279>
1222

1223 Fiechter, J., Rose, K. A., Curchitser, E. N. & Hedstrom, K. S. (2015). The role of environmental
1224 controls in determining sardine and anchovy population cycles in the California Current:
1225 Analysis of an end-to-end model. *Progress in Oceanography*, 138, 381-398.
1226 <https://doi.org/10.1016/j.pocean.2014.11.013>
1227

1228 Field, J. C., Baltz, K. E. N., Phillips, A. J., & Walker, W. A. (2007). Range expansion and
1229 trophic interactions of the jumbo squid, *Dosidicus gigas*, in the California Current.
1230 *California Cooperative Oceanic Fisheries Investigations Report*, 48, 131-146.
1231

- 1232 Franks, P. J. (2001). Turbulence avoidance: An alternate explanation of turbulence-enhanced
1233 ingestion rates in the field. *Limnology and Oceanography*, 46(4), 959-963.
1234 <https://doi.org/10.4319/lo.2001.46.4.0959>
1235
- 1236 Freeland, H. J. (2006). What proportion of the North Pacific Current finds its way into the Gulf
1237 of Alaska? *Atmosphere-Ocean*, 44(4), 321-330. <https://doi.org/10.3137/ao.440401>
1238
- 1239 Gaube, P., Braun, C. D., Lawson, G. L., McGillicuddy, D. J., Della Penna, A., Skomal, G. B., ...
1240 & Thorrold, S. R. (2018). Mesoscale eddies influence the movements of mature female
1241 white sharks in the Gulf Stream and Sargasso Sea. *Scientific reports*, 8(1), 1-8.
1242 <https://doi.org/10.1038/s41598-018-25565-8>
1243
- 1244 Godefroid, M., Boldt, J. L., Thorson, J. T., Forrest, R., Gauthier, S., Flostrand, L., ... &
1245 Galbraith, M. (2019). Spatio-temporal models provide new insights on the biotic and
1246 abiotic drivers shaping Pacific Herring (*Clupea pallasii*) distribution. *Progress in*
1247 *Oceanography*, 178, 102198. <https://doi.org/10.1016/j.pocean.2019.102198>
1248
- 1249 Goericke, R., Venrick, E., Mantyla, A., Hoof, R., Collins, C., Gaxiola-Castro, G., ... & Sydeman,
1250 W. J. (2005). The state of the California Current, 2004-2005: still cool? *California*
1251 *Cooperative Oceanic Fisheries Investigations Report*, 46, 32-71.
1252
- 1253 Grandin, C. J., Johnson, K. F., Edwards, A. M., & Berger, A. M. (2020). Status of the Pacific
1254 Hake (whiting) stock in U.S. and Canadian waters in 2020. Prepared by the Joint
1255 Technical Committee of the U.S. and Canada Pacific Hake/Whiting Agreement, National
1256 Marine Fisheries Service and Fisheries and Oceans Canada. 273 p.
1257
- 1258 Haltuch, M. A., Tolimieri, N., Lee, Q., & Jacox, M. G. (2020). Oceanographic drivers of petrale
1259 sole recruitment in the California Current Ecosystem. *Fisheries Oceanography*, 29(2),
1260 122-136. <https://doi.org/10.1111/fog.12459>
1261
- 1262 Harden Jones, F. R. (1968). Fish migration. St. Martin's Press, New York.
1263
- 1264 Hare, J. A. (2014). The future of fisheries oceanography lies in the pursuit of multiple
1265 hypotheses. *ICES Journal of Marine Science*, 71(8), 2343-2356.
1266
- 1267 Hare, J. A., & Cowen, R. K. (1996). Transport mechanisms of larval and pelagic juvenile
1268 bluefish (*Pomatomus saltatrix*) from South Atlantic Bight spawning grounds to Middle
1269 Atlantic Bight nursery habitats. *Limnology and Oceanography*, 41(6), 1264-1280.
1270 <https://doi.org/10.4319/lo.1996.41.6.1264>
1271
- 1272 Hare, S. R., Mantua, N. J. & Francis, R. C. (1999). Inverse production regimes: Alaska and
1273 west coast Pacific salmon. *Fisheries*, 24(1), 6-14.
1274
- 1275 Hickey, B. M. (1989). Patterns and Processes of Circulation over the Washington Continental
1276 Shelf and Slope, 41-115. In: *Coastal Oceanography of Washington and Oregon*. Landry
1277 M. R., & Hickey, B. M. (Eds.), Elsevier Science, Amsterdam, The Netherlands.

1278 [https://doi.org/10.1016/S0422-9894\(08\)70346-5](https://doi.org/10.1016/S0422-9894(08)70346-5)
1279
1280 Hickey, B. M. (1998). Coastal oceanography of western North America, from the tip of Baja
1281 California to Vancouver Island. *The sea*, 11, 1062.
1282
1283 Hickey, B. M., & Banas, N. S. (2008). Why is the northern end of the California Current System
1284 so productive? *Oceanography*, 21(4), 90-107. <http://www.jstor.org/stable/24860012>
1285
1286 Hickey, B., Geier, S., Kachel, N., & MacFadyen, A. (2005). A bi-directional river plume: The
1287 Columbia in summer. *Continental Shelf Research* 25(14): 1,631-1,656.
1288 <https://doi.org/10.1016/j.csr.2005.04.010>
1289
1290 Hinckley, S., Hermann, A. J., & Megrey, B. A. (1996). Development of a spatially explicit,
1291 individual-based model of marine fish early life history. *Marine Ecology Progress Series*,
1292 139, 47-68. doi:10.3354/meps139047
1293
1294 Hjort, J. (1914). Fluctuations in the great fisheries of Northern Europe. Rappports et Proces-
1295 verbaux des Reunions, Conseil International pour l'Exploration de la Mer, 20, 1-13.
1296
1297 Hjort, J. (1926). Fluctuation in the year classes of important food fishes. Journal du Conseil/
1298 Conseil Permanent International pour l'Exploration de la Mer, 1, 5-38.
1299
1300 Hollowed, A. B. (1992). Spatial and temporal distributions of Pacific hake, *Merluccius*
1301 *productus*, larvae and estimates of survival during early life stages. *California*
1302 *Cooperative Oceanic Fisheries Investigations Report*, 33, 100-123.
1303
1304 Hollowed, A. B., & Bailey, K. M. (1989). New perspectives on the relationship between
1305 recruitment of Pacific hake (*Merluccius productus*) and the ocean environment. In:
1306 Effects of ocean variability on recruitment and an evaluation of parameters used in stock
1307 assessment models. Beamish R. J., & McFarlane, G. A. (Eds). *Canadian Special*
1308 *Publication of Fisheries and Aquatic Sciences*, 108, 207-220.
1309
1310 Hollowed, A. B., Bond, N. A., Wilderbuer, T. K., Stockhausen, W. T., A'mar, Z. T., Beamish, R.
1311 J., ... & Schirripa, M. J. (2009). A framework for modelling fish and shellfish responses
1312 to future climate change. *ICES Journal of Marine Science*, 66(7), 1584-1594.
1313 <https://doi.org/10.1093/icesjms/fsp057>
1314
1315 Hollowed, A. B., Hare, S. R., & Wooster, W. S. (2001). Pacific Basin climate variability and
1316 patterns of Northeast Pacific marine fish production. *Progress in Oceanography*, 49(1-4),
1317 257-282. [https://doi.org/10.1016/S0079-6611\(01\)00026-X](https://doi.org/10.1016/S0079-6611(01)00026-X)
1318
1319 Horne, J. K., & Smith, P. E. (1997). Space and time scales in Pacific hake recruitment processes:
1320 latitudinal variation over annual cycles. *California Cooperative Oceanic Fisheries*
1321 *Investigations Report*, 38, 90-102.
1322
1323 Houde, E. D. (1987). Fish early life dynamics and recruitment variability. *American Fisheries*

1324 *Society Symposium*, 2, 17-29.
1325

1326 Houde, E. D. (1997). Patterns and trends in larval-stage growth and mortality of teleost fish.
1327 *Journal of Fish Biology*, 51, 52-83. <https://doi.org/10.1111/j.1095-8649.1997.tb06093.x>
1328

1329 Huyer, A. (1983). Coastal upwelling in the California Current system. *Progress in*
1330 *Oceanography*, 12(3), 259-284. [https://doi.org/10.1016/0079-6611\(83\)90010-1](https://doi.org/10.1016/0079-6611(83)90010-1)
1331

1332 Huyer, A., Sobey, E. J. C., & R. L. Smith (1979). The spring transition in currents over the
1333 Oregon continental shelf. *Journal of Geophysical Research*, 84, 6995-7011.
1334 <https://doi.org/10.1029/JC084iC11p06995>
1335

1336 Jacobsen, N. S., Berger, A. M., Marshall, K. N., & Taylor, I. G. (2019). A management strategy
1337 evaluation of Pacific Hake: implications of spatial distribution and differentiated harvest
1338 control rules. DRAFT for submission to Scientific Review Group.
1339

1340 Jacobsen, N. S., Marshall, K. N., Berger, A. M., Grandin, C. J., & Taylor, I. G. (2021).
1341 Management Strategy Evaluation of Pacific Hake: Exploring the Robustness of the
1342 Current Harvest Policy to Spatial Stock Structure, Shifts in Fishery Selectivity, and
1343 Climate-Driven Distribution Shifts. NOAA Technical Memorandum NMFS-NWFSC-
1344 168. <https://doi.org/10.25923/x9f9-9b20>
1345

1346 Jacox, M. G., Alexander, M. A., Siedlecki, S., Chen, K., Kwon, Y. O., Brodie, S., ... &
1347 Capotondi, A. (2020). Seasonal-to-interannual prediction of North American coastal
1348 marine ecosystems: Forecast methods, mechanisms of predictability, and priority
1349 developments. *Progress in Oceanography*, 183, 102307.
1350 <https://doi.org/10.1016/j.pocean.2020.102307>
1351

1352 Jacox, M. G., Alexander, M. A., Stock, C. A., & Hervieux, G. (2017). On the skill of seasonal
1353 sea surface temperature forecasts in the California Current System and its connection to
1354 ENSO variability. *Climate Dynamics*, 53, 7519–7533.
1355 <https://doi.org/10.1007/s00382-017-3608-y>
1356

1357 Jacox, M. G., Bograd, S. J., Hazen, E. L., & Fiechter, J. (2015). Sensitivity of the California
1358 Current nutrient supply to wind, heat, and remote ocean forcing. *Geophysical Research*
1359 *Letters*, 42, 5950-5957. <https://doi.org/10.1002/2015GL065147>
1360

1361 Jacox, M. G., Edwards, C. A., Hazen, E. L., & Bograd, S. J. (2018). Coastal upwelling revisited:
1362 Ekman, Bakun, and improved upwelling indices for the US West Coast. *Journal of*
1363 *Geophysical Research: Oceans*, 123(10), 7332-7350.
1364 <https://doi.org/10.1029/2018JC014187>
1365

1366 Jacox, M. G., Fiechter, J., Moore, A. M., & Edwards, C. A. (2015). ENSO and the California
1367 Current coastal upwelling response. *Journal of Geophysical Research: Oceans*, 120,
1368 1691-1702. <https://doi.org/10.1002/2014JC010650>
1369

- 1370 Jacox, M. G., Hazen, E. L., & Bograd, S. J. (2016). Optimal environmental conditions and
1371 anomalous ecosystem responses: Constraining bottom-up controls of phytoplankton
1372 biomass in the California current system. *Scientific Reports*, 6, 27612.
1373 <https://doi.org/10.1038/srep27612>
1374
- 1375 Jacox, M. G., Moore, A. M., Edwards, C. A., & Fiechter, J. (2014). Spatially resolved upwelling
1376 in the California Current System and its connections to climate variability. *Geophysical*
1377 *Research Letters*, 41, 3189–3196. <https://doi.org/10.1002/2014GL059589>
1378
- 1379 Kaplan, I. C., Williams, G. D., Bond, N. A., Hermann, A. J., & Siedlecki, S. A. (2016). Cloudy
1380 with a chance of sardines: Forecasting sardine distributions using regional climate
1381 models. *Fisheries Oceanography*, 25, 15–27. <https://doi.org/10.1111/fog.12131>
1382
- 1383 Keister, J. E., Di Lorenzo, E., Morgan, C. A., Combes, V. & Peterson, W. T. (2011).
1384 Zooplankton species composition is linked to ocean transport in the Northern California
1385 Current. *Global Change Biology*, 17(7), 2498-2511.
1386
- 1387 Laake, J. L., Lowry, M. S., DeLong, R. L., Melin, S. R., & Carretta, J. V. (2018). Population
1388 growth and status of California sea lions. *The Journal of Wildlife Management*, 82(3),
1389 583-595. <https://doi.org/10.1002/jwmg.21405>
1390
- 1391 Laine, P., & Rajasilta, M. (1999). The hatching success of Baltic herring eggs and its relation to
1392 female condition. *Journal of Experimental Marine Biology and Ecology*, 237(1), 61-73.
1393 [https://doi.org/10.1016/S0022-0981\(98\)00213-5](https://doi.org/10.1016/S0022-0981(98)00213-5)
1394
- 1395 Landry, F., Miller, T. J. and Leggett, W. C. (1995). The effects of small-scale turbulence on the
1396 ingestion rate of fathead minnow (*Pimephales promelas*) larvae. *Canadian Journal of*
1397 *Fisheries and Aquatic Sciences*, 52(8), 1714-1719.
1398
- 1399 Lasker, R. (1978). The relation between oceanographic conditions and larval anchovy food in
1400 the California Current: identification of factors contributing to recruitment failure.
1401 Rapports et Proces-verbaux des Réunions. Conseil International pour l'Exploration de la
1402 Mer, 173, 212-230.
1403
- 1404 Lasker, R. (1981). The role of a stable ocean in larval fish survival and subsequent recruitment.
1405 *Marine fish larvae: morphology, ecology and relation to fisheries*, 1, 80-89.
1406
- 1407 Litz, M. N., Phillips, A. J., Brodeur, R. D., & Emmett, R. L. (2011). Seasonal occurrences of
1408 Humboldt squid (*Dosidicus gigas*) in the northern California Current System. *California*
1409 *Cooperative Oceanic Fisheries Investigations Report*, 52, 97-108.
1410
- 1411 Litzow, M. A., Ciannelli, L., Puerta, P., Wettstein, J. J., Rykaczewski, R. R., & Opiekun, M.
1412 (2018). Non-stationary climate–salmon relationships in the Gulf of Alaska. *Proceedings*
1413 *of the Royal Society B*, 285(1890), 20181855. <https://doi.org/10.1098/rspb.2018.1855>
1414

- 1415 Livingston, P. A., & Bailey, K. M. (1985). Trophic role of the Pacific whiting, *Merluccius*
1416 *productus*. *Marine Fisheries Review*, 47(2), 16-22.
1417
- 1418 Lo, N. C. (2007). Daily larval production of Pacific hake (*Merluccius productus*) off California
1419 in 1951-2006. *California Cooperative Oceanic Fisheries Investigations Report*, 48, 147.
1420
- 1421 Logerwell, E. A., & Smith, P. E. (2001). Mesoscale eddies and survival of late stage Pacific
1422 sardine (*Sardinops sagax*) larvae. *Fisheries Oceanography*, 10(1), 13-25.
1423 <https://doi.org/10.1046/j.1365-2419.2001.00152.x>
1424
- 1425 Lynn, R. J., & Simpson, J. J. (1987). The California Current System: The seasonal variability of
1426 its physical characteristics. *Journal of Geophysical Research: Oceans*, 92(C12), 12947-
1427 12966. <https://doi.org/10.1029/JC092iC12p12947>
1428
- 1429 Mackas, D. L., Thomson, R. E., & Galbraith, M. (2001). Changes in the zooplankton community
1430 of the British Columbia continental margin, 1985-1999, and their covariation with
1431 oceanographic conditions. *Canadian Journal of Fisheries and Aquatic Sciences*, 58(4),
1432 685-702. <https://doi.org/10.1139/f01-009>
1433
- 1434 MacKenzie, B. R., & Leggett, W. C. (1991). Quantifying the contribution of small-scale
1435 turbulence to the encounter rates between larval fish and their zooplankton prey: effects
1436 of wind and tide. *Marine Ecology Progress Series*, 73(2), 149-160.
1437 <https://www.int-res.com/articles/meps/73/m073p149.pdf>
1438
- 1439 MacKenzie, B. R., Miller, T. J., Cyr, S., & Leggett, W. C. (1994). Evidence for a dome-shaped
1440 relationship between turbulence and larval fish ingestion rates. *Limnology and*
1441 *Oceanography*, 39(8), 1790-1799. <https://doi.org/10.4319/lo.1994.39.8.1790>
1442
- 1443 Malick, M. J., Adkison, M. D., & Wertheimer, A. C. (2009). Variable effects of biological and
1444 environmental processes on coho salmon marine survival in Southeast Alaska.
1445 *Transactions of the American Fisheries Society*, 138(4), 846-860.
1446 <https://doi.org/10.1577/T08-177.1>
1447
- 1448 Malick, M. J., Cox, S. P., Peterman, R. M., Wainwright, T. C., & Peterson, W. T. (2015).
1449 Accounting for multiple pathways in the connections among climate variability, ocean
1450 processes, and coho salmon recruitment in the Northern California Current. *Canadian*
1451 *Journal of Fisheries and Aquatic Sciences*, 72(10), 1552-1564.
1452 <https://doi.org/10.1139/cjfas-2014-0509>
1453
- 1454 Malick, M. J., Cox, S. P., Mueter, F. J., Dorner, B., & Peterman, R. M. (2017). Effects of the
1455 North Pacific Current on the productivity of 163 Pacific salmon stocks. *Fisheries*
1456 *Oceanography*, 26(3), 268-281. <https://doi.org/10.1111/fog.12190>
1457
- 1458 Malick, M. J., Hunsicker, M. E., Haltuch, M. A., Parker-Stetter, S. L., Berger, A. M., &
1459 Marshall, K. N. (2020). Relationships between temperature and Pacific hake distribution

1460 vary across latitude and life-history stage. *Marine Ecology Progress Series*, 639, 185-
1461 197. DOI: <https://doi.org/10.3354/meps13286>

1462

1463 Mantua, N. J., Hare, S. R., Zhang, Y., Wallace, J. M., & Francis, R. C. (1997). A Pacific
1464 interdecadal climate oscillation with impacts on salmon production. *Bulletin of the*
1465 *American Meteorological Society*, 78(6), 1069-1080.
1466 [https://doi.org/10.1175/1520-0477\(1997\)078<1069:APICOW>2.0.CO;2](https://doi.org/10.1175/1520-0477(1997)078<1069:APICOW>2.0.CO;2)

1467

1468 Matarese, A. C., Kendall Jr., A. W., Blood, D. M., & Vinter, B. M. (1989). Laboratory guide to
1469 early life history stages of northeast Pacific fishes. U.S. Department of Commerce,
1470 NOAA Technical Report. NMFS 80, 632 pp.

1471

1472 McFarlane, G. A., & Beamish, R. J. (1992). Climatic influence linking copepod production with
1473 strong year-classes in sablefish, *Anoplopoma fimbria*. *Canadian Journal of Fisheries and*
1474 *Aquatic Sciences*, 49, 743-753. <https://doi.org/10.1139/f92-083>

1475

1476 Mendelsohn, R., Schwing, F. B., & Bograd, S. J. (2003). Spatial structure of subsurface
1477 temperature variability in the California Current, 1950-1993. *Journal of Geophysical*
1478 *Research: Oceans*, 108(C3). <https://doi.org/10.1029/2002JC001568>

1479

1480 Moore, A. M., Jacox, M. G., Crawford, W. J., Laughlin, B., Edwards, C. A., & Fiechter, J.
1481 (2017). The impact of the ocean observing system on estimates of the California
1482 Current Circulation spanning three decades. *Progress in Oceanography*, 156, 41-60.
1483 <https://doi.org/10.1016/j.pocean.2017.05.009>

1484

1485 Myers, R. A. (1998). When do environment–recruitment correlations work? *Reviews in Fish*
1486 *Biology and Fisheries*, 8(3), 285-305. <https://doi.org/10.1023/A:1008828730759>

1487

1488 Nelson, M. O., & Larkins, H. A. (1970). Distribution and biology of Pacific hake: a synopsis. In:
1489 Pacific hake, p. 23-33. U.S. Fish and Wildlife Service, Circular 332.
1490 <https://spo.nmfs.noaa.gov/sites/default/files/legacy-pdfs/CIRC332.pdf>

1491

1492 Neveu, E., Moore, A. M., Edwards, C. A., Fiechter, J., Drake, P., Crawford, W. J., ... & Nuss, E.
1493 (2016). An historical analysis of the California Current circulation using ROMS 4D-Var:
1494 System configuration and diagnostics. *Ocean Modelling*, 99, 133-151.
1495 <https://doi.org/10.1016/j.ocemod.2015.11.012>

1496

1497 Owen, R. W. (1980). Eddies of the California Current System: Physical and Ecological
1498 Characteristics. In: *2nd California Islands Multidisciplinary Symposium*. 1978. 237-263.
1499 National Park Service. <http://hdl.handle.net/10139/2881>

1500

1501 Pepin, P. (1991). Effect of temperature and size on development, mortality, and survival rates of
1502 the pelagic early life history stages of marine fish. *Canadian Journal of Fisheries and*
1503 *Aquatic Sciences*, 48(3), 503-518. <https://doi.org/10.1139/f91-065>

1504

1505 Peterman, R. M., & Bradford, M. J. (1987). Wind speed and mortality rate of a marine fish, the
1506 northern anchovy (*Engraulis mordax*). *Science*, 235(4786), 354-356.

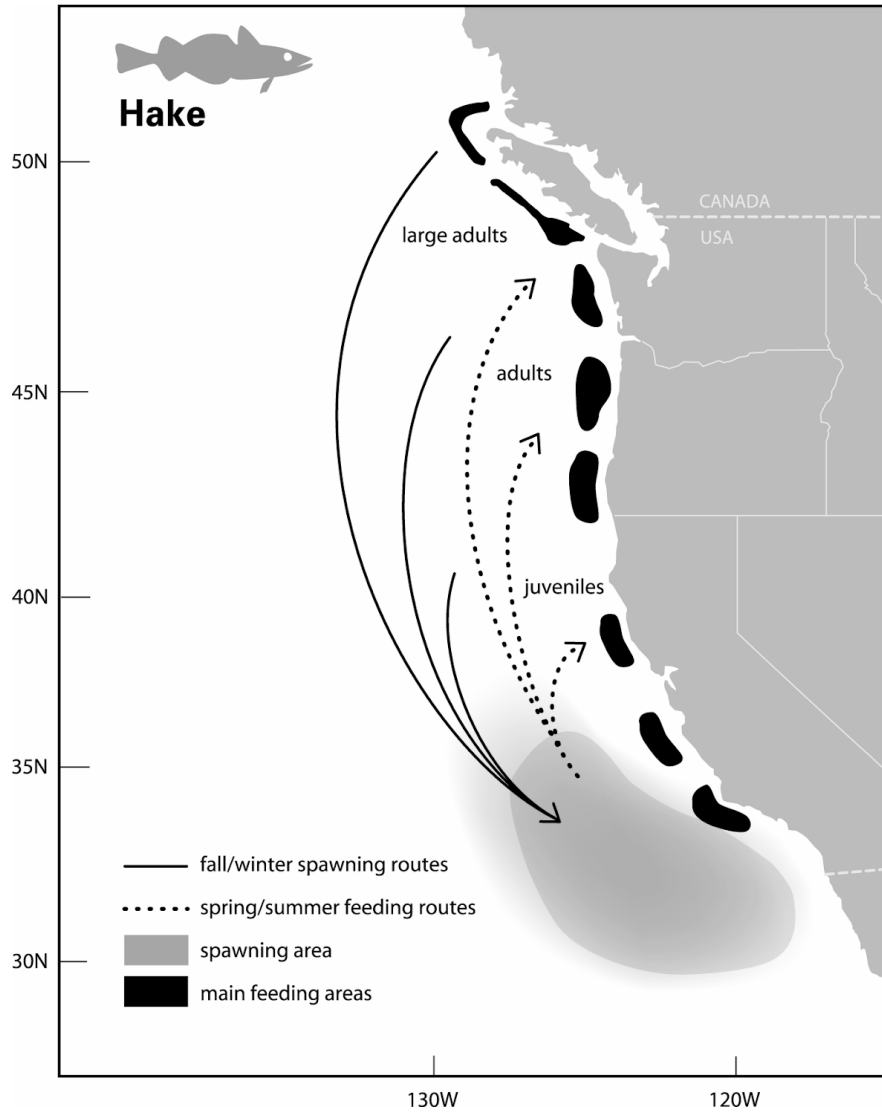
1507 DOI: 10.1126/science.235.4786.354
1508
1509 Peterson, W. T. (2009). Copepod species richness as an indicator of longterm changes in the
1510 coastal ecosystem of the northern *California Current*. *California Cooperative Oceanic*
1511 *Fisheries Investigations Reports*, 50, 73-81.
1512
1513 Peterson, W. T., & Keister, J. E. (2003). Interannual variability in copepod community
1514 composition at a coastal station in the northern California Current: a multivariate
1515 approach. *Deep Sea Research Part II: Topical Studies in Oceanography*, 50(14-16),
1516 2499-2517.
1517
1518 Phillips, A. J., Ralston, S., Brodeur, R. D., Auth, T. D., Emmett, R. L., Johnson, C., &
1519 Wespestad, V. G. (2007). Recent pre-recruit Pacific hake (*Merluccius productus*)
1520 occurrences in the northern California Current suggest a northward expansion of their
1521 spawning area. *California Cooperative Oceanic Fisheries Investigations Report*, 48, 215-
1522 229.
1523
1524 Phillips, E. M. (2022). Spatiotemporal variability of euphausiids in the California Current
1525 Ecosystem: Insights from a recently developed time series. *ICES Journal of Marine*
1526 *Science*. <https://doi.org/10.1093/icesjms/fsac055>
1527
1528 Pörtner, H. O., Berdal, B., Blust, R., Brix, O., Colosimo, A., De Wachter, B., ... & Zakhartsev,
1529 M. (2001). Climate induced temperature effects on growth performance, fecundity and
1530 recruitment in marine fish: developing a hypothesis for cause and effect relationships in
1531 Atlantic cod (*Gadus morhua*) and common eelpout (*Zoarces viviparus*). *Continental*
1532 *Shelf Research*, 21(18-19), 1975-1997. [https://doi.org/10.1016/S0278-4343\(01\)00038-3](https://doi.org/10.1016/S0278-4343(01)00038-3)
1533
1534 Pozo Buil, M., Jacox, M. G., Fiechter, J., Alexander, M. A., Bograd, S. J., Curchitser, E. N.,
1535 Edwards, C. A., Rykaczewski, R. R., & Stock, C. A. (2021). A dynamically downscaled
1536 ensemble of future projections for the California Current System. *Frontiers in Marine*
1537 *Science*, 8, p.324. <https://doi.org/10.3389/fmars.2021.612874>
1538
1539 Reiss, C. S., Checkley Jr, D. M., & Bograd, S. J. (2008). Remotely sensed spawning habitat of
1540 Pacific sardine (*Sardinops sagax*) and Northern anchovy (*Engraulis mordax*) within the
1541 California Current. *Fisheries Oceanography*, 17(2), 126-136.
1542 <https://doi.org/10.1111/j.1365-2419.2008.00469.x>
1543
1544 Ressler, P. H., Holmes, J. A., Fleischer, G. W., Thomas, R. E., & Cooke, K. C. (2007). Pacific
1545 hake, *Merluccius productus*, Autecology: a timely review. *Marine Fisheries Review*,
1546 69(1), 1.
1547
1548 Rijnsdorp, A. D., Berghahn, R., Miller, J. M., & Van der Veer, H. W. (1995). Recruitment
1549 mechanisms in flatfish: what did we learn and where do we go? *Netherlands Journal of*
1550 *Sea Research*, 34(1-3), 237-242. [https://doi.org/10.1016/0077-7579\(95\)90031-4](https://doi.org/10.1016/0077-7579(95)90031-4)
1551

- 1552 Rodgveller, C. J., Stark, J. W., Echave, K. B. & Hulson, P. J. F. (2016). Age at maturity, skipped
1553 spawning, and fecundity of female sablefish (*Anoplopoma fimbria*) during the spawning
1554 season. *Fishery Bulletin*, 114(1).
1555
- 1556 Roughgarden, J., Pennington, J. T., Stoner, D., Alexander, S., & Miller, K. (1991). Collisions of
1557 upwelling fronts with the intertidal zone: the cause of recruitment pulses in barnacle
1558 populations of central California. *Acta oecologica*, 12(1), 35-51.
1559
- 1560 R Core Team (2020). R: A language and environment for statistical computing. R Foundation for
1561 Statistical Computing, Vienna, Austria. <http://www.R-project.org/>
1562
- 1563 Saha, S., Moorthi, S., Pan, H. L., Wu, X., Wang, J., Nadiga, S., ... & Goldberg, M. (2010). The
1564 NCEP climate forecast system reanalysis. *Bulletin of the American Meteorological*
1565 *Society*, 91(8), 1015-1058. <https://doi.org/10.1175/2010BAMS3001.1>
1566
- 1567 Sakuma, K. M., & Ralston, S. (1997). Vertical and horizontal distribution of juvenile Pacific
1568 whiting (*Merluccius productus*) in relation to hydrography off California. *California*
1569 *Cooperative Oceanic Fisheries Investigations Report*, 38, 137-146.
- 1570 Sampson, D. B., Hamel, O. S., Bosley, K., Budrick, J., Cronin-Fine, L., Hillier, L. K., Hinton, K.
1571 E., Krigbaum, M. J., Miller, S., Privitera-Johnson, K. M., Ramey, K., Rodomsky, B. T.,
1572 Solinger, L. K., & Whitman, A. D. (2017). 2017 Assessment Update for the US West
1573 Coast Stock of Arrowtooth Flounder. Pacific Fishery Management Council, Portland,
1574 OR. Available from <http://www.pcouncil.org/groundfish/stock-assessments/>
1575
- 1576 Sánchez, F., & Gil, J. (2000). Hydrographic mesoscale structures and Poleward Current as a
1577 determinant of hake (*Merluccius merluccius*) recruitment in southern Bay of
1578 Biscay. *ICES journal of Marine Science*, 57(1), 152-170.
1579 <https://doi.org/10.1006/jmsc.1999.0566>
1580
- 1581 Schirripa, M. J., & Colbert, J. J. (2006). Interannual changes in sablefish (*Anoplopoma fimbria*)
1582 recruitment in relation to oceanographic conditions within the California Current System.
1583 *Fisheries Oceanography*, 15, 25-36. <https://doi.org/10.1111/j.1365-2419.2005.00352.x>
1584
- 1585 Schweigert, J. F., Hay, D. E., Therriault, T. W., Thompson, M., & Haegele, C. W. (2009).
1586 Recruitment forecasting using indices of young-of-the-year Pacific herring (*Clupea*
1587 *pallasii*) abundance in the Strait of Georgia (BC). *ICES journal of Marine Science*, 66,
1588 1681-1687. <https://doi.org/10.1093/icesjms/fsp182>
1589
- 1590 Shanks, A. L., & Morgan, S. G. (2018). Testing the intermittent upwelling hypothesis:
1591 upwelling, downwelling, and subsidies to the intertidal zone. *Ecological Monographs*,
1592 88(1), 22-35. <https://doi.org/10.1002/ecm.1281>
1593
- 1594 Siedlecki, S. A., Banas, N. S., Davis, K. A., Giddings, S., Hickey, B. M., MacCready, P.,
1595 Connolly, T., & Geier, S. (2015). Seasonal and interannual oxygen variability on the
1596 Washington and Oregon continental shelves, *Journal of Geophysical Research: Oceans*,
1597 120, 608-633. <https://doi.org/10.1002/2014JC010254>

1598
1599 Siedlecki, S. A., Kaplan, I. C., Hermann, A. J., Nguyen, T. T., Bond, N. A., Newton, J. A., ... &
1600 Feely, R. A. (2016). Experiments with seasonal forecasts of ocean conditions for the
1601 northern region of the California Current upwelling system. *Scientific Reports*, 6, 27203.
1602 <https://doi.org/10.1038/srep27203>
1603
1604 Smith, P. E. (1995). Development of the population biology of the Pacific hake, *Merluccius*
1605 *productus*. *California Cooperative Oceanic Fisheries Investigations Report*, 36, 144-152.
1606
1607 Smith, B. D., McFarlane, G. A., & Saunders, M. W. (1990). Variation in Pacific hake
1608 (*Merluccius productus*) summer length-at-age near southern Vancouver Island and its
1609 relationship to fishing and oceanography. *Canadian Journal of Fisheries and Aquatic*
1610 *Sciences*, 47(11), 2195-2211. <https://doi.org/10.1139/f90-244>
1611
1612 Sogard, S. M., Berkeley, S. A., & Fisher, R. (2008). Maternal effects in rockfishes *Sebastes* spp.:
1613 a comparison among species. *Marine Ecology Progress Series*, 360, 227-236.
1614 <https://doi.org/10.3354/meps07468>
1615
1616 Stauffer, G. D. (1985). Biology and life history of the coastal stock of Pacific whiting,
1617 *Merluccius productus*. *Marine Fisheries Review*, 47(2), 2-7.
1618 <https://spo.nmfs.noaa.gov/sites/default/files/pdf-content/MFR/mfr472/mfr4722.pdf>
1619
1620 Strub, P. T., & James, C. (2000). Altimeter-derived variability of surface velocities in the
1621 California Current System: 2. Seasonal circulation and eddy statistics. *Deep Sea*
1622 *Research Part II: Topical Studies in Oceanography*, 47(5-6), 831-870.
1623 [https://doi.org/10.1016/S0967-0645\(99\)00129-0](https://doi.org/10.1016/S0967-0645(99)00129-0)
1624
1625 Sumida, B. Y., & Moser, H. G. (1980). Food and feeding of Pacific hake larvae, *Merluccius*
1626 *productus*, off southern California and northern Baja California. *California Cooperative*
1627 *Oceanic Fisheries Investigations Report*, 21, 161-166.
1628 https://calcofi.com/publications/calcofireports/v21/Vol_21_Sumida_Moser.pdf
1629
1630 Sundby, S. (1991). Factors affecting the vertical distribution of eggs. *ICES Journal of Marine*
1631 *Science*, 192, 33-38.
1632
1633 Swartzman, G. (2001). Spatial patterns of Pacific hake (*Merluccius productus*) shoals and
1634 euphausiid patches in the California Current ecosystem. *Spatial Processes and*
1635 *Management of Marine Populations*, 495-512.
1636
1637 Sydeman, W. J., Thompson, S. A., Field, J. C., Peterson, W. T., Tanasichuk, R. W., Freeland, H.
1638 J., Bograd, S. J., & Rykaczewski, R. R. (2011). Does positioning of the North Pacific
1639 Current affect downstream ecosystem productivity? *Geophysical Research*
1640 *Letters*, 38(12). <https://doi.org/10.1029/2011GL047212>
1641
1642 Thompson, R. E. (1981). Oceanography of the British Columbia coast. *Canadian Special*
1643 *Publication of Fisheries and Aquatic Sciences*, 56. 291 p.

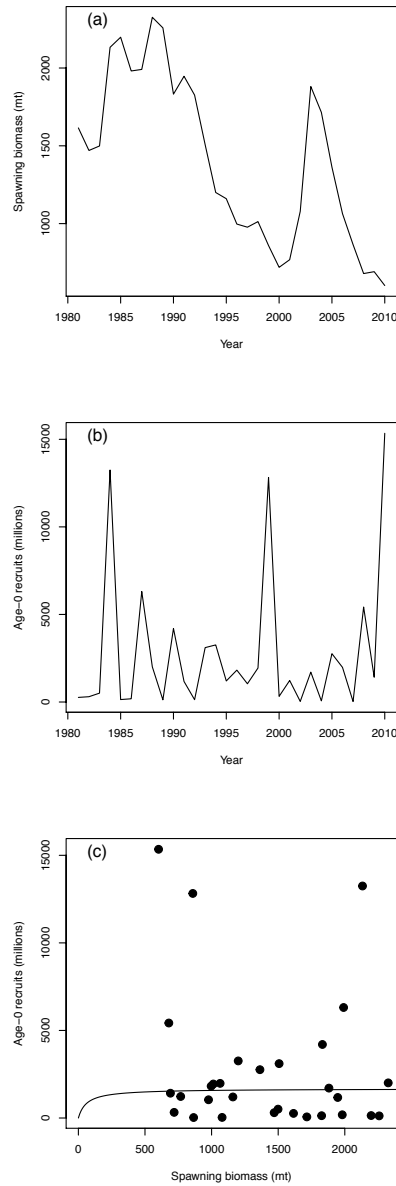
1644
1645 Tillman, M. F. (1968). Tentative recommendations for management of the coastal fishery
1646 of Pacific hake, based on a simulation study of the effects of fishing upon a virgin
1647 population (Doctoral dissertation, MS thesis), University of Washington, Seattle, WA.
1648
1649 Tommasi, D., Stock, C. A., Pegion, K., Vecchi, G. A., Methot, R. D., Alexander, M. A.
1650 & Checkley Jr., D. M. (2017). Improved management of small pelagic fisheries
1651 through seasonal climate prediction. *Ecological Applications*, 27(2), 378-388.
1652 <https://doi.org/10.1002/eap.1458>
1653
1654 Tolimieri, N., & Levin, P. S. (2005). The Roles of Fishing and Climate in the Population
1655 Dynamics of Bocaccio Rockfish. *Ecological Applications*, 15, 458-468.
1656 <https://doi.org/10.1890/03-5376>
1657
1658 Tolimieri, N., Haltuch, M. A., Lee, Q., Jacox, M. G., & Bograd, S. J. (2018). Oceanographic
1659 drivers of sablefish recruitment in the California Current. *Fisheries Oceanography*, 27(5),
1660 458-474. <https://doi.org/10.1111/fog.12266>
1661
1662 Trenberth, K. E. (1997). The definition of El Niño. *Bulletin of the American Meteorological*
1663 *Society*, 78(12), 2771-2778.
1664 [https://doi.org/10.1175/1520-0477\(1997\)078<2771:TDOENO>2.0.CO;2](https://doi.org/10.1175/1520-0477(1997)078<2771:TDOENO>2.0.CO;2)
1665
1666 Turley, B. D., & Rykaczewski, R. R. (2019). Influence of wind events on larval fish mortality
1667 rates in the southern California Current Ecosystem. *Canadian Journal of Fisheries and*
1668 *Aquatic Sciences*, 76(12), 2418-2432. <https://doi.org/10.1139/cjfas-2018-0458>
1669
1670 Van Der Kraak, G., & Pankhurst, N. W. (1997). Temperature effects on the reproductive
1671 performance of fish. In: 'Global Warming: Implications for Freshwater and Marine
1672 Fish'. Wood, C. M., & McDonald, D. G. (Eds). pp. 159-176.
1673
1674 Van der Veer, H. W., Berghahn, R., Miller, J. M., & Rijnsdorp, A. D. (2000). Recruitment in
1675 flatfish, with special emphasis on North Atlantic species: progress made by the Flatfish
1676 Symposia. *ICES Journal of Marine Science*, 57(2), 202-215.
1677 <https://doi.org/10.1006/jmsc.1999.0523>
1678
1679 Van Holmes, C. (2007). Mean Spring and Fall Upwelling Transition Dates off the Oregon and
1680 Washington Coasts.
1681 <http://www.cbr.washington.edu/sites/default/files/papers/trans.cbrmean.pdf>
1682
1683 Vastano, A. C., Incze, L. S., & Schumacher, J. D. (1992). Observation and analysis of fishery
1684 processes: larval pollock at Shelikof Strait, Alaska. *Fisheries Oceanography*, 1(1), 20-31.
1685 <https://doi.org/10.1111/j.1365-2419.1992.tb00022.x>
1686
1687 Veneziani, M., Edwards, C. A., Doyle, J. D., & Foley, D. (2009). A central California coastal
1688 ocean modeling study: 1. Forward model and the influence of realistic versus
1689 climatological forcing. *Journal of Geophysical Research*, 114, C04015.

1690 <https://doi.org/10.1029/2008JC004774>
1691
1692 Venrick, E. L., Bograd, S. J., Checkley, D. A., Durazo, R. E., Gaxiola-Castro, G. I., Hunter, J.
1693 O., Huyer, A. D., Hyrenbach, K. D., Laveniegos, B. E., Mantyla, A. R., & Schwing, F. B.
1694 (2003). The state of the California Current, 2002-2003: Tropical and subarctic influences
1695 vie for dominance. *California Cooperative Oceanic Fisheries Investigations Report*, 44,
1696 28-60.
1697
1698 Vestfals, C. D., Ciannelli, L., Duffy-Anderson, J. T., & Ladd, C. (2014). Effects of seasonal and
1699 interannual variability in along-shelf and cross-shelf transport on groundfish recruitment
1700 in the eastern Bering Sea. *Deep Sea Research Part II: Topical Studies in Oceanography*,
1701 109, 190-203. <https://doi.org/10.1016/j.dsr2.2013.09.026>
1702
1703 Ware, D. M., & McFarlane, G. A. (1986). Relative impact of Pacific hake, sablefish and Pacific
1704 cod on west coast of Vancouver Island herring stocks. *International North Pacific*
1705 *Fisheries Commission Bulletin*, 47, 67-78.
1706
1707
1708 Ware, D. M., & McFarlane, G. A. (1995). Pelagic community interactions in the Vancouver
1709 Island upwelling system. *Climate Change and Northern Fish Populations*, 121, 509-521.
1710 Beamish, R. J. (Ed.). NRC Research Press.
1711
1712 Wilderbuer, T. K., Hollowed, A. B., Ingraham Jr, W. J., Spencer, P. D., Conners, M. E., Bond,
1713 N. A., & Walters, G. E. (2002). Flatfish recruitment response to decadal climatic
1714 variability and ocean conditions in the eastern Bering Sea. *Progress in Oceanography*,
1715 55(1-2), 235-247. [https://doi.org/10.1016/S0079-6611\(02\)00081-2](https://doi.org/10.1016/S0079-6611(02)00081-2)
1716
1717 Woodbury, D., Hollowed, A. B., & Pearce, J. A. (1995). Interannual variation in growth rates
1718 and back-calculated spawn dates of juvenile Pacific hake (*Merluccius productus*). *Belle*
1719 *W. Baruch Library in Marine Science*, 19, 481-496.
1720
1721 Zabel, R. W., Levin, P. S., Tolimieri, N., & Mantua, N. J. (2011). Interactions between climate
1722 and population density in the episodic recruitment of bocaccio, *Sebastes paucispinis*, a
1723 Pacific rockfish. *Fisheries Oceanography* 20, 294-304.
1724 <https://doi.org/10.1111/j.1365-2419.2011.00584.x>



1727
1728
1729
1730
1731
1732
1733
1734
1735
1736
1737
1738
1739
1740
1741
1742

FIGURE 1: Hypothesized movement and spatial population structure of Pacific hake (*Merluccius productus*), reproduced from Agostini et al. (2006).



1744

1745

1746

1747

1748

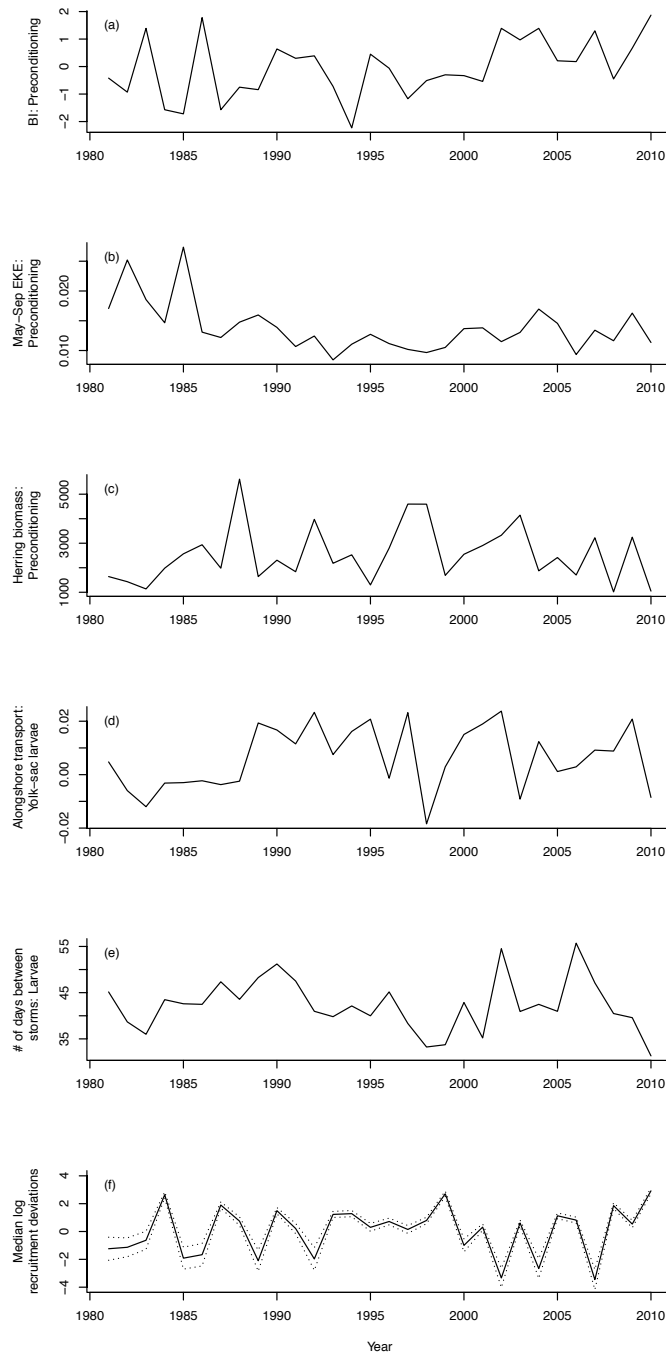
1749

1750

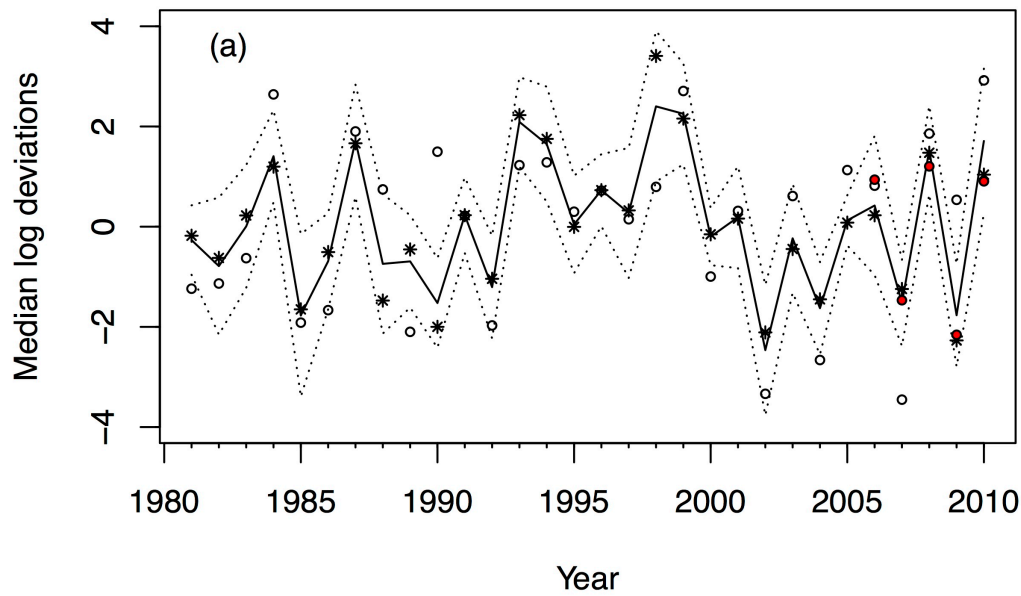
1751

1752

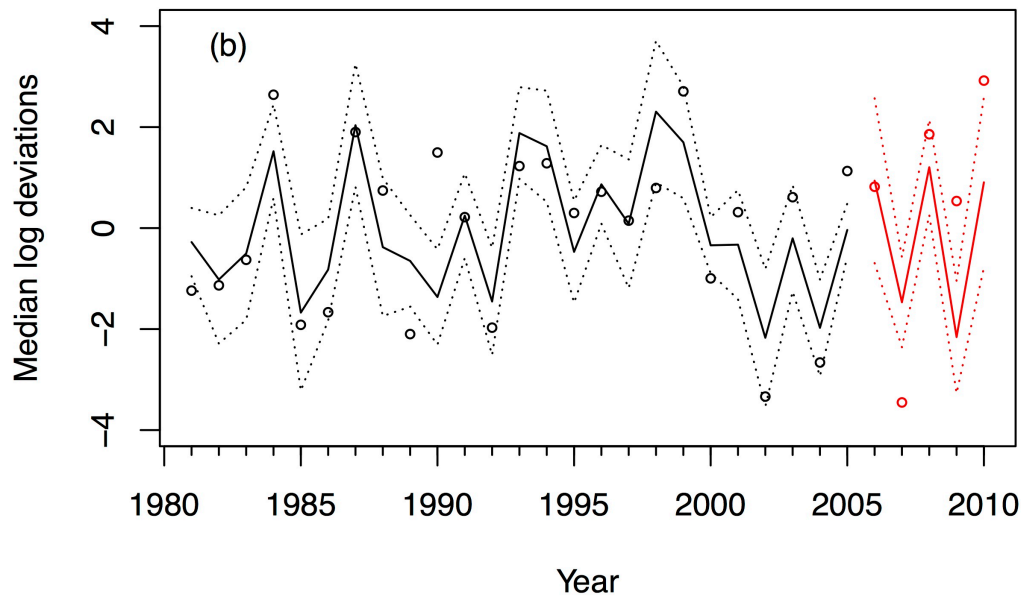
FIGURE 2: Derived quantities of Pacific hake (*Merluccius productus*) from the 2020 stock assessment (Grandin et al., 2020) for 1981 – 2010: (a) spawning stock biomass (SSB) in metric tons (mt), (b) age-0 recruits in millions, and (c) the stock-recruitment relationship supported in the assessment (line) versus observed data (points). Values for unfished recruitment (R_0) = 1600, steepness (h) = 0.854, and unfished female spawning biomass (B_0 , thousand t) = 1,385 were obtained from Table 27 in the 2020 assessment.



1753
 1754 FIGURE 3: Time series of independent predictor variables in the AIC-best model of Pacific hake
 1755 (*Merluccius productus*) recruitment: (a) bifurcation index (BI), (b) May – September eddy
 1756 kinetic energy (EKE) between 34.5° and 42.5°N, and (c) Pacific herring (*Clupea pallasii*)
 1757 biomass off the west coast of Canada during the adult female preconditioning stage, (d)
 1758 alongshore transport during the yolk-sac larval stage, and (e) number of days between storm
 1759 events during the first-feeding larval stage compared to (f) median log recruitment deviations
 1760 from the 2020 Pacific hake stock assessment (Grandin et al., 2020). Dotted lines are ± 1.0
 1761 standard deviation (*SD*).



1762



1763

1764

1765 FIGURE 4: (a) Fit of the AIC-best model ($R^2 = 0.59$) to the estimated median log recruitment
 1766 deviations from the 2020 Pacific hake (*Merluccius productus*) stock assessment. Solid line is the
 1767 predicted recruitment deviations from the full time series. Dotted lines = 95% confidence limits.

1768 Open circles are the median log recruitment deviations from the 2020 Pacific hake assessment.

1769 Stars are predicted values from jackknife analysis removing individual years one at a time. Red

1770 points are predictions from fitting the AIC-best model to 1981–2005 and then predicting 2006–

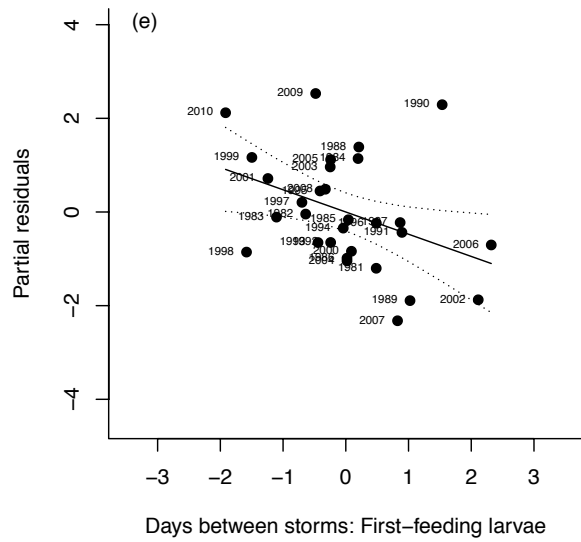
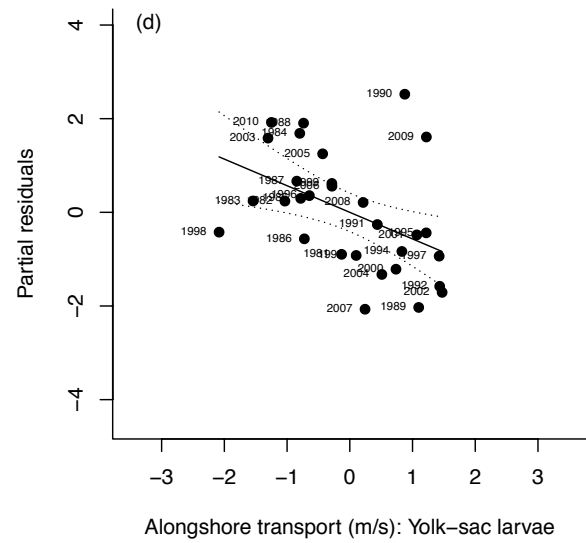
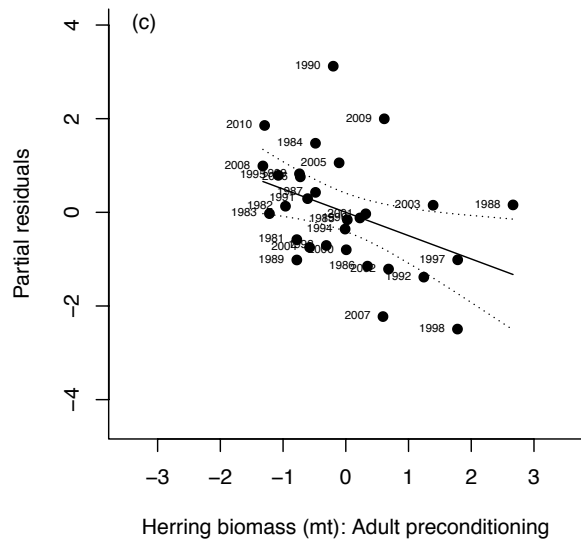
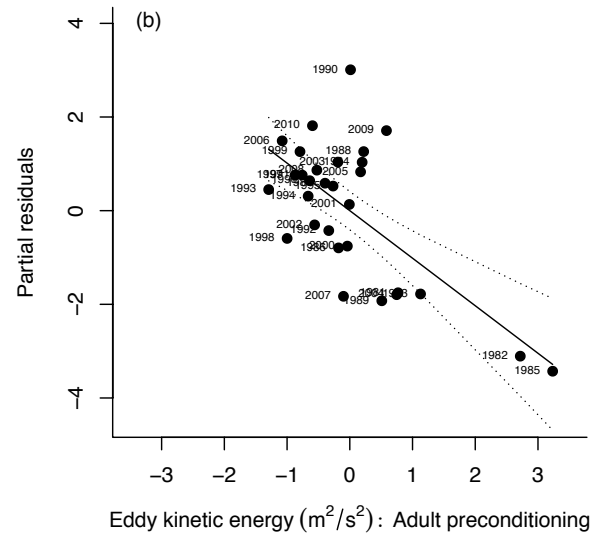
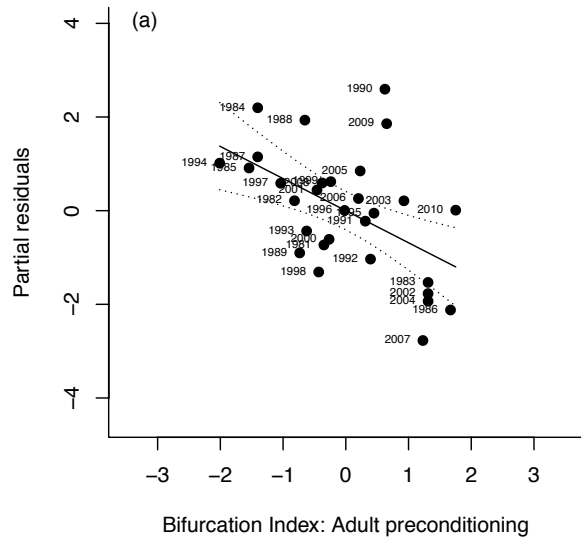
1771 2010. (b) Fit of the AIC-best model from jackknife-refitting the 1981–2005 data ($R^2 = 0.63$).

1772 Open circles are the log recruitment deviations from the 2020 Pacific hake assessment. Solid

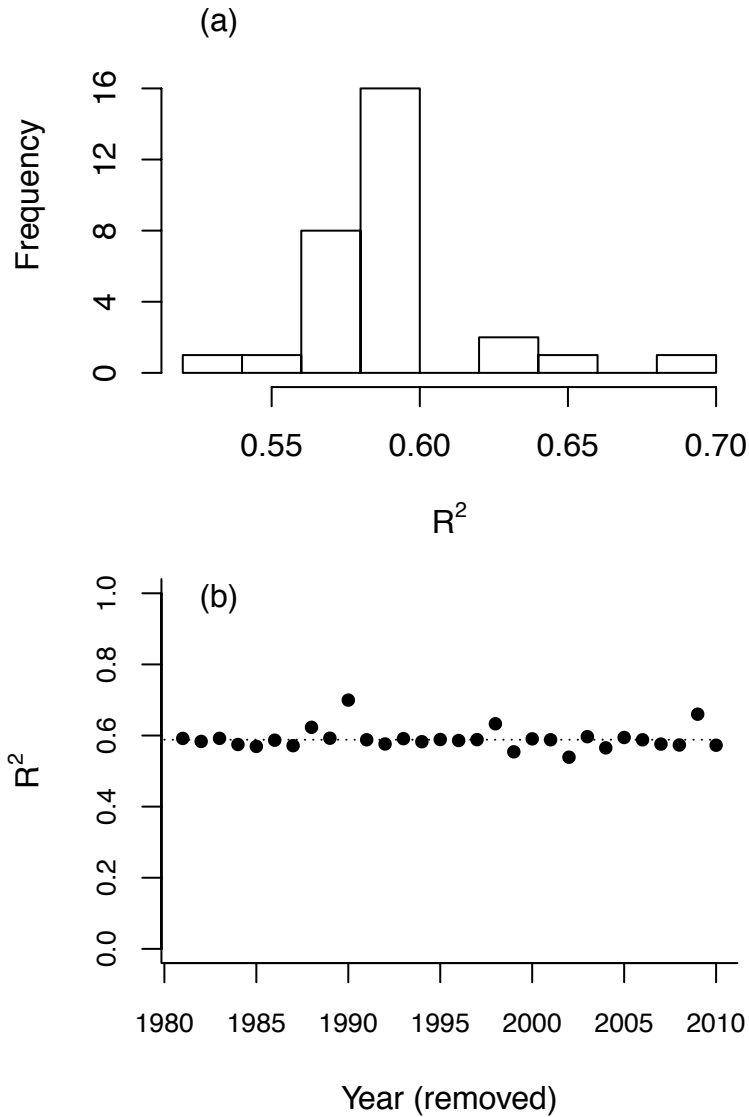
1773 black line is the predicted recruitment deviations from the model for 1981–2005; solid red line is

1774 the predicted recruitment deviations for 2006–2010 based on the model for 1981–2005. Dotted

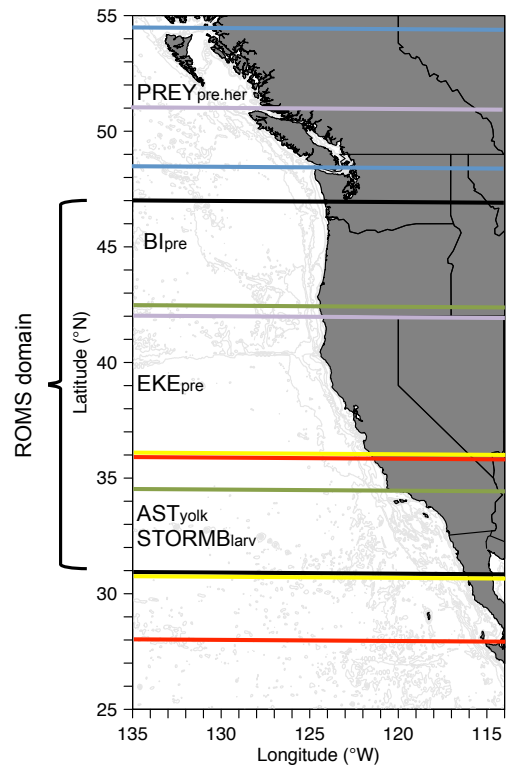
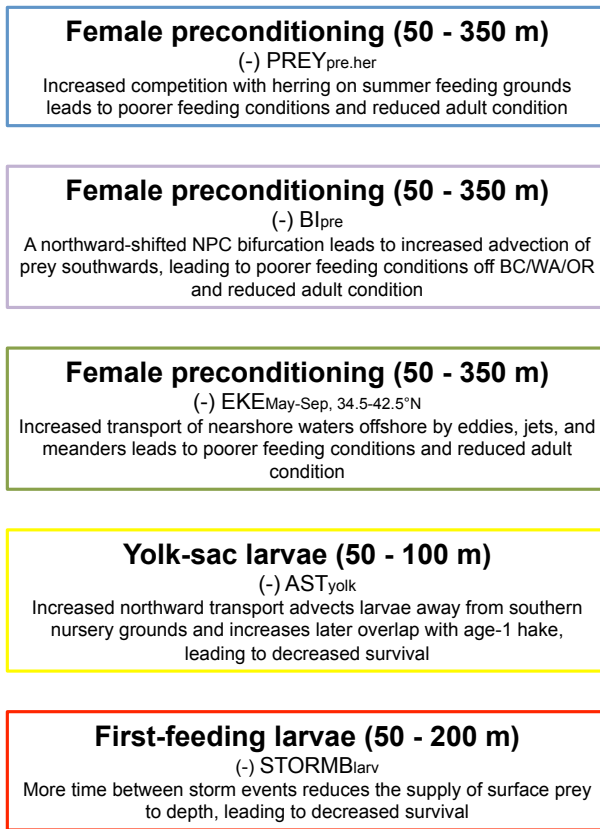
1775 lines = 95% confidence limits.



1778 FIGURE 5: Partial residual plots of predictor variables in the the AIC-best model of Pacific hake
 1779 (*Merluccius productus*) recruitment: (a) the bifurcation index, (b) May – September eddy kinetic
 1780 energy (EKE) between 34.5° and 42.5°N, and (c) Pacific herring (*Clupea pallasii*) biomass off
 1781 the west coast of Canada during the adult female preconditioning stage, (d) alongshore transport
 1782 during the yolk-sac larval stage, and (e) number of days between storm events during the first-
 1783 feeding larval stage.



1784
 1785 FIGURE 6: Results of jackknife resampling showing the distribution of R^2 values. (a) Frequency
 1786 distribution of R^2 values, and (b) R^2 for when the indicated year was removed from the model.
 1787
 1788
 1789
 1790



1791
 1792
 1793
 1794
 1795
 1796
 1797
 1798
 1799
 1800
 1801
 1802
 1803
 1804

FIGURE 7: Conceptual model for Pacific hake (*Merluccius productus*) showing the environmental drivers at specific life-history stages that lead to higher recruitment. Signs in parentheses indicate the partial correlation of each term with residuals from the Pacific hake stock-recruitment relationship. See Figure 4 for plots of these relationships. Boundary lines correspond to the region over which the predictor was calculated.

1805 TABLE 1: Pacific hake (*Merluccius productus*) conceptual life history model showing spatiotemporally-explicit hypotheses by life
 1806 stage related to factors (covariates) affecting survival. The adult female preconditioning through yolk-sac larval stages are shown here.
 1807 For full conceptual life history model, see TABLE A1.

Ho Number	Life-history stage	Time period	Hypothesis	Stage	Covariates	Depth	Longitudinal extent	Latitudinal extent	Source
H1	Preconditioning	Apr - Oct (Year 0)	(H1) Higher temperature increases food demand resulting in lower egg production, egg quality, or probability of spawning and lowers recruitment	TEMP _{pre}	Mean temperature	50 - 350 m	Shelf break, between 100 - 2000 m isobaths	42° - 47°N	ROMS
H2			(H2) As (H1), but degree days, not mean temperature	DD _{pre}	Degree days	50 - 350 m	Shelf break, between 100 - 2000 m isobaths	42° - 47°N	ROMS
H3			(H3) Higher coastal upwelling leads to increased productivity, better condition, higher egg production, egg quality, or probability of spawning and increases recruitment	UW _{pre.c}	Coastal upwelling (CUTI)	Base of mixed layer		41.5° - 47.5°N	Jacox et al. (2018), https://oceanview.pfeg.noaa.gov
H4			(H4) As (H3), but biologically effective upwelling	UW _{pre.b}	Biologically effective upwelling (BEUTI)	Base of mixed layer	0 - 75 km offshore	41.5° - 47.5°N	Jacox et al. (2018), https://oceanview.pfeg.noaa.gov
H5			(H5) Food availability affects energy allocation to reproduction with higher recruitment when more prey are available during the preconditioning period	PREY _{pre.her} PREY _{pre.juwhake}	Index of age-0 and age-1 Pacific hake biomass, and age-2 Pacific herring biomass				Stock assessments
H6			(H6) Timing of availability of food affects energy allocation to reproduction with higher recruitment when more prey are available during the preconditioning period	SPT _{pre}	Mean date of the spring transition from downwelling-favorable southerly winds to upwelling-favorable northerly winds		125°W	42°N (West of OR/CA border) 45°N (West of Siletz Bay, OR) 48°N (West of La Push, WA)	CBR Mean Method, Van Holmes (2007), http://www.cbr.washington.edu/status/trans
H7	Spawning	Jan - Mar	(H7) Temperature acts as a spawning cue with fish less likely to spawn at high temperature resulting in lower recruitment	TEMP _{spawn}	Mean temperature	130 - 500 m	Shelf break, between 100 - 2000 m isobaths	31° - 36°N	ROMS
H8			(H8) As (H7), but degree days, not mean temperature	DD _{spawn}	Degree days	130 - 500 m	Shelf break, between 100 - 2000 m isobaths	31° - 36°N	ROMS
H9	Eggs	Jan - Mar	(H9) Eggs aggregate at base of mixed layer so Mixed Layer Depth may limit how far they rise in the water column affecting later transport	MLD _{eggs}	Mean mixed layer depth (m)		Shelf break, between 100 - 2000 m isobaths	31° - 36°N	ROMS
H10			(H10) Transport to settlement habitat affects recruitment (transport varies with latitude)	CST _{eggs.s} CST _{eggs.n}	Net cross-shelf transport	40 - 60 m	Shelf break, between 100 - 2000 m isobaths	31° - 34.5°N 34.5° - 36°N	ROMS
H11			(H11) Increased northward advection away from juvenile nursery areas decreases recruitment	AST _{eggs}	Net alongshore transport	40 - 60 m	Shelf break, between 100 - 2000 m isobaths	31° - 36°N	ROMS
H12			(H12) Increased northward advection away from juvenile nursery areas decreases recruitment	PU _{eggs}	Strength of the poleward undercurrent	75 - 275 m	Coast to 275 m isobath	32.5° - 33.5°N	ROMS
H13			(H13) Growth/Predation hypothesis: growth rate is faster in warm water leading to reduced time vulnerable to predators	DD _{eggs}	Degree days	40 - 60 m	Shelf break, between 100 - 2000 m isobaths	31° - 36°N	ROMS
H14	Yolk-sac larvae	Jan - Apr	(H14) Larvae aggregate at base of mixed layer so Mixed Layer Depth may limit how far they rise in the water column affecting later transport	MLD _{yolk}	Mean mixed layer depth (m)		Shelf break, between 100 - 2000 m isobaths	31° - 36°N	ROMS
H15			(H15) Transport to settlement habitat affects recruitment (transport varies with latitude)	CST _{yolk.s} CST _{yolk.n}	Net cross-shelf transport	50 - 100 m	Shelf break, between 100 - 2000 m isobaths	31° - 34.5°N 34.5° - 36°N	ROMS
H16			(H16) Increased northward advection away from juvenile nursery areas decreases recruitment	AST _{yolk}	Net alongshore transport				ROMS
H17			(H17) Increased northward advection away from juvenile nursery areas decreases recruitment	PU _{yolk}	Strength of the poleward undercurrent	75 - 275 m	Coast to 275 m isobath	32.5° - 33.5°N	ROMS
H18			(H18) Growth/Predation hypothesis: growth rate is faster in warm water leading to reduced time vulnerable to predators	DD _{yolk}	Degree days	50 - 100 m		31° - 36°N	ROMS

1809 TABLE 2: The set of top candidate models (those with $\Delta AICc < 3.0$) that were used to identify factors influencing Pacific hake
 1810 (*Merluccius productus*) early life history survival and recruitment. Models are ordered by $\Delta AICc$, so the overall best model, as
 1811 supported by the data, is identified as Model 1.
 1812

Model															R^2	$\Delta AICc$	
1	ASTyolk	BIpre	-	EKEpre.MS.c	-	-	-	-	-	PREYpre.her	-	-	STORMBlarv	-	-	0.59	0.00
2	ASTyolk	BIpre	-	EKEpre.MS.c	-	-	-	-	-	PREYpre.her	-	-	-	-	-	0.52	1.03
3	-	-	CALMlarv	EKEpre.MS.c	PREDage0.age1.hake	-	-	-	-	-	-	-	-	-	UWpre.cu	0.51	1.70
4	ASTyolk	BIpre	-	EKEpre.MS.c	-	-	-	-	-	-	-	-	STORMBlarv	-	-	0.51	1.75
5	-	-	CALMlarv	EKEpre.MS.c	-	-	-	-	-	-	-	-	-	-	UWpre.cu	0.46	1.79
6	ASTyolk	BIpre	-	EKEpre.MS.c	-	-	PDOpre	-	-	PREYpre.her	-	-	-	-	-	0.56	2.05
7	ASTyolk	BIpre	-	EKEpre.MS.c	-	-	-	-	-	-	-	-	-	-	-	0.45	2.17
8	ASTyolk	BIpre	-	EKEpre.MS.c	-	-	NPGOpre.AS	-	-	PREYpre.her	-	-	-	-	-	0.56	2.19
9	-	-	CALMlarv	EKEpre.MS.c	PREDage0.age1.hake	-	-	-	-	-	-	-	STORMDlarv	UWpre.cu	0.56	2.20	
10	ASTyolk	BIpre	-	EKEpre.MS.c	-	-	PDOpre	-	-	-	-	-	-	-	-	0.50	2.23
11	ASTyolk	BIpre	-	EKEpre.MS.c	-	-	-	-	-	PREYpre.her	-	SPTRpre	-	-	-	0.55	2.41
12	-	BIpre	-	EKEpre.MS.c	-	-	-	-	-	PREYpre.her	-	-	STORMBlarv	-	-	0.50	2.59
13	ASTyolk	BIpre	-	EKEpre.MS.c	-	-	-	-	-	PREYpre.her	-	-	-	STORMDlarv	-	0.55	2.59
14	ASTyolk	BIpre	CALMlarv	EKEpre.MS.c	-	-	-	-	-	PREYpre.her	-	-	-	-	-	0.55	2.61
15	-	-	-	EKEpre.MS.c	-	-	-	PREYlatelarv.eup	-	-	-	STORMBlarv	STORMDlarv	UWpre.cu	0.55	2.88	
16	-	-	CALMlarv	EKEpre.MS.c	-	-	-	-	-	SPTR	-	-	-	UWpre.cu	0.49	2.94	

1813
 1814
 1815 *Note:* Abbreviations: AS, April – September; AST, alongshore transport; BI, bifurcation index; c, central region from 34.5 – 42.5°N;
 1816 CALM, number of calm periods; cu, Coastal Upwelling Transport Index (CUTI); EKE, eddy kinetic energy; larv, first-feeding larval
 1817 stage; latelarv, late larval stage; MS, May – September; NPGO, North Pacific Gyre Oscillation; PDO, Pacific Decadal Oscillation; pre,
 1818 preconditioning stage; PREDage0.age1.hake, log-transformed predation of age-0 Pacific hake (*Merluccius productus*) by age-1 hake;
 1819 PREY eup, euphausiids as prey for late larval stages; PREY her, Pacific herring (*Clupea pallasii*) as prey for adult female
 1820 preconditioning stage; SPTR, timing of spring transition; STORMB, number of days between storm events; STORMD, duration of
 1821 storm events; UW, upwelling; yolk, yolk-sac larval stage.

1822 TABLE 3: Coefficients for the AIC-best model of Pacific hake (*Merluccius productus*)
 1823 recruitment (Model 1 in Table 2) showing both raw and standardized (beta) coefficients.

	Coefficient	Bias	SE	Standardized Coefficient	Std Bias	Std SE
Intercept	8.26	0.03	2.05	0.04	0.00	0.23
BI_{pre}	-0.63	-0.02	0.21	-0.69	-0.03	0.23
EKE_{pre.MS.c}	-242.70	-0.65	57.34	-1.02	0.00	0.24
PREY_{pre.her}	0.00	0.00	0.00	-0.50	0.02	0.23
AST_{yolk}	-47.88	-1.68	20.72	-0.57	-0.02	0.25
STORMB_{larv}	-0.08	0.00	0.04	-0.47	-0.01	0.24

1824 *Note:* Bias and standard error (*SE*) are from bootstrap resampling. Abbreviations: AST,
 1825 alongshore transport; BI, bifurcation index; c, central region from 34.5 - 42.5°N; CALM,
 1826 number of calm periods; EKE, eddy kinetic energy; larv, first-feeding larval stage; MS,
 1827 May – September; pre, preconditioning stage; PREY_{her}, Pacific herring (*Clupea pallasii*)
 1828 as prey during preconditioning stage; STORMB, number of days between storm events.

1829
 1830
 1831
 1832
 1833

1834 TABLE 4: Correlations among variables in the AIC-best model of Pacific hake
 1835 (*Merluccius productus*) recruitment.

1836

	BI_{pre}	EKE_{pre.MS.c}	PREY_{pre.her}	AST_{yolk}	STORMB_{larv}	VIF
BI_{pre}	-					1.03
EKE_{pre.MS.c}	-0.14	-				1.09
PREY_{pre.her}	-0.06	-0.17	-			1.04
AST_{yolk}	-0.01	-0.19	0.04	-		1.15
STORMB_{larv}	0.02	-0.06	-0.02	0.31	-	1.11

1837
 1838
 1839
 1840
 1841
 1842
 1843

Note: Abbreviations: AST, alongshore transport; BI, bifurcation index; c, central region from 34.5 - 42.5°N; CALM, number of calm periods; EKE, eddy kinetic energy; larv, first-feeding larval stage; MS, May – September; pre, preconditioning stage; PREY_{her}, Pacific herring (*Clupea pallasii*) as prey during preconditioning stage; STORMB, number of days between storm events; VIF, variance inflation factor.

1844 TABLE 5: Variables included in all candidate models of Pacific hake (*Merluccius*
 1845 *productus*) recruitment from jackknife refits of the entire model-fitting process. Bolded
 1846 variables were those found in the AIC-best model.

Predictor	Number of times included	%
AST_{yolk}	25	40
BI	1	2
BI_{pre}	34	55
CALM_{larv}	23	37
CST _{larv.s}	0	0
CST ² _{larv.s}	0	0
CST _{latelarv.s}	1	2
CST ² _{latelarv.s}	1	2
EKEMS.c	1	2
EKE_{pre.MS.c}	59	95
logPRED _{age0.age1.hake}	5	8
ONIAS	0	0
ONI _{pre}	0	0
NPGOAS	1	2
NPGO _{pre.AS}	1	2
PDOJA	0	0
PDOAS	0	0
PDO _{pre}	1	2
PRED _{age0.atf}	0	0
PRED _{age0.csl}	0	0
PREY _{larv.zp}	0	0
PREY _{latelarv.eup}	6	10
PREY _{pre.her}	7	11
SPTR	1	2
SPTR _{pre}	0	0
STORM _{larv}	1	2
STORMB_{larv}	13	21
STORMD _{larv}	4	6
UW _{pre.cu}	25	40
Total number of models	62	

1847 *Note:* Results are the number of years a specific predictor was in the best-fit model
 1848 (lowest AICc and fewest parameters). Individual years could have more than one
 1849 candidate model.

1850 Abbreviations: age-0, age-0 pelagic juvenile stage; age1, age-1 pelagic juvenile stage;
1851 AS, April – September; AST, alongshore transport; BI, bifurcation index; c, central
1852 region from 34.5 - 42.5°N; CALM, number of calm events; CALMB, number of days
1853 between calm events; CALMD, duration of calm events; CST, cross-shelf transport at
1854 depths of 50 – 300 m; EKE, eddy kinetic energy; eup, euphausiids; JA, January – April;
1855 larv, first-feeding larval stage; latelarv, late larval stage; NPGO, North Pacific Gyre
1856 Oscillation; ONI, Ocean Niño Index; PDO, Pacific Decadal Oscillation; pre,
1857 preconditioning stage; PREDage0.age1.hake; predation of age-0 hake by age-1 hake;
1858 PREDage0.atf, predation of age-0 hake by arrowtooth flounder; PREDage0.csl, predation
1859 of age-0 hake by California sea lions; PREYlarv.zp, copepods as prey for first-feeding
1860 (and late) larvae; PREYlatelarv.eup, euphausiids as prey for late larvae; PREYpre.her,
1861 Pacific herring as prey for adult female preconditioning stage; s, southern region from
1862 31.0 °- 34.5°N; SPTR, Julian day of spring transition; STORM, number of storm events;
1863 STORMB, number of days between storm events; STORMD, duration of storm events;
1864 UW, coastal upwelling; yolk, yolk-sac larval stage; zp, copepod zooplankton.
1865
1866
1867
1868
1869
1870
1871
1872
1873
1874
1875
1876
1877
1878
1879
1880
1881
1882
1883
1884
1885
1886
1887
1888
1889
1890
1891
1892
1893
1894
1895

1896 TABLE 6: Results from completely refitting the model 100 times while jackknife
 1897 resampling median recruitment deviations from a log-normal distribution using the
 1898 recruitment deviations and SDs from the 2020 Pacific hake (*Merluccius productus*) stock
 1899 assessment.

Predictor	Number of jackknives	Number of models	%
AST_{yolk}	48	65	41
BI	0	0	0
BI_{pre}	54	72	46
CALM _{larv}	52	70	44
CST _{larv.s}	2	2	1
CST ² _{larv.s}	1	1	1
CST _{latelarv.s}	7	7	4
CST ² _{latelarv.s}	3	3	2
EKEMS.c	1	1	1
EKE_{pre.MS.c}	87	128	81
logPRED _{age0.age1.hake}	19	21	13
ONIAS	0	0	0
ONI _{pre}	0	0	0
NPGOAS	0	0	0
NPGO _{pre.AS}	4	4	3
PDOJA	8	12	8
PDOAS	2	3	2
PDO _{pre}	10	10	6
PRED _{age0.atf}	1	1	1
PRED _{age0.csl}	0	0	0
PREY _{larv.zp}	3	3	2
PREY _{latelarv.eup}	7	8	5
PREY _{pre.her}	23	27	17
SPTR	9	13	8
SPTR _{pre}	2	2	1
STORM _{larv}	0	0	0
STORMB_{larv}	21	23	15
STORMD _{larv}	4	5	3
UW _{pre.cu}	48	63	40
Total	100	158	

1900 *Note:* Each refit iteration could include multiple candidate models (with AICc < 2.0 and
1901 the fewest included parameters). Number of jackknives is the number of times the
1902 variable was included in one of the candidate models for any jackknife iteration. Number
1903 of models is the total number of times the variable was included in a model across all
1904 candidate models. Total is the total number of jackknife iterations and the total number of
1905 models fit. See Table 5 for an explanation of ROMS parameters. Bold text indicates
1906 variables from the AIC-best model.
1907

1908

1909

1910

1911

1912

1913

1914

1915

1916

1917

1918

1919

1920

1921

1922

1923

1924

1925

1926

1927

1928

1929

1930

1931

1932

1933

1934

1935

1936

1937

1938

1939

1940

1941

1942

1943

1944

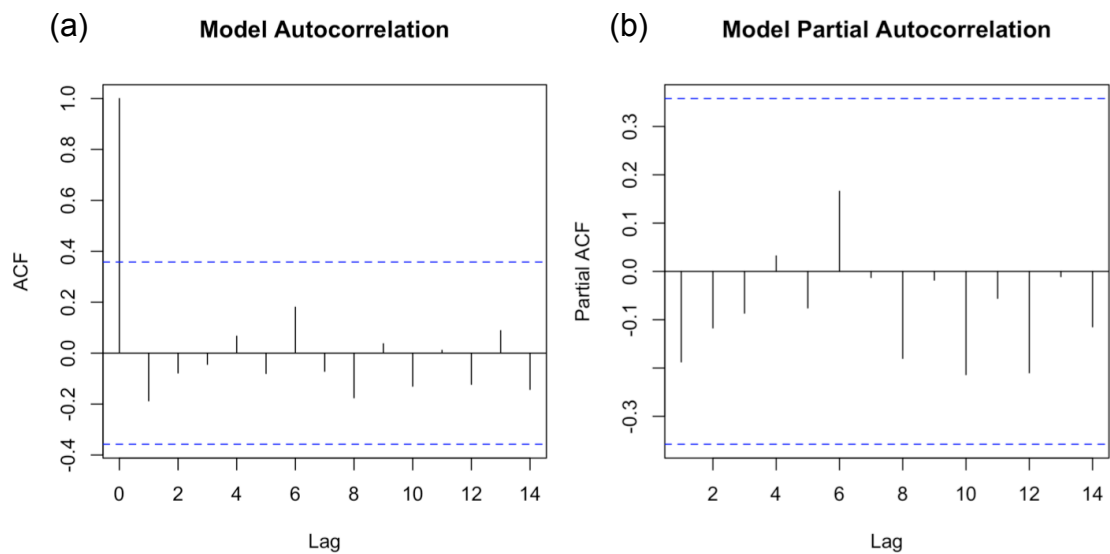
1945

1946

1947 TABLE 7: The number of times each predictor variable was included in model fits of
 1948 data (1981 – 2005) across the jackknife resampling procedure.
 1949

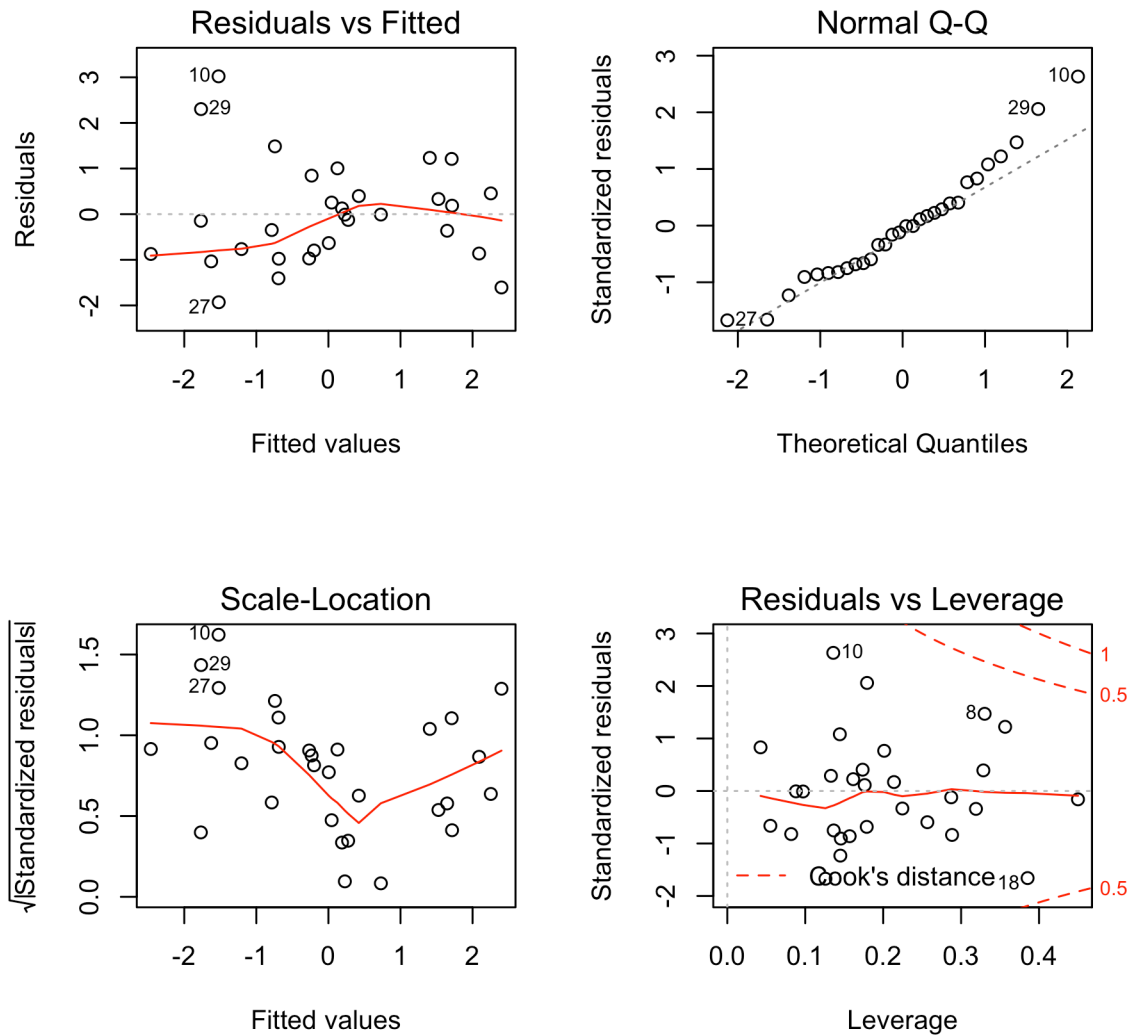
Predictor	Times included	%
AST _{yolk}	2	5
BI	0	0
BI _{pre}	23	55
CALM _{larv}	10	24
CST _{larv.s}	32	76
CST ² _{larv.s}	30	71
CST _{latelarv.s}	0	0
CST ² _{latelarv.s}	0	0
EKEMS.c	0	0
EKE _{pre.MS.c}	3	7
logPRED _{age0.age1.hake}	41	98
ONIAS	4	10
ONI _{pre}	26	62
NPGOAS	2	5
NPGO _{pre.AS}	4	10
PDOJA	2	5
PDOAS	0	0
PDO _{pre}	1	2
PRED _{age0.atf}	14	33
PRED _{age0.csl}	2	5
PREY _{larv.zp}	0	0
PREY _{latelarv.eup}	3	7
PREY _{pre.her}	1	2
SPTR	0	0
SPTR _{pre}	0	0
STORM _{larv}	1	2
STORMB _{larv}	0	0
STORMD _{larv}	0	0
UW _{pre.cu}	6	14

1950 Note: Times included is the number of times the AIC-best model (AICc < 2.0, fewest
 1951 parameters) included the term. There was only one AIC-best model for each year
 1952 iteration. See Table 5 for an explanation of ROMS parameters.
 1953



1956
1957
1958
1959
1960
1961

FIGURE A1: Autocorrelation Function (ACF) and Partial Autocorrelation Function (PACF) plots of the residuals for the AIC-best model of Pacific hake (*Merluccius productus*) recruitment. Blue dashed lines indicate the 95% confidence intervals.



1968
 1969 FIGURE A3: AIC-best model diagnostic plots showing (a) residuals vs. fitted values, (b)
 1970 normal Q-Q plot, (c) scale-location, and (d) residuals vs. leverage.
 1971

1972
 1973 TABLE A1: Pacific hake (*Merluccius productus*) conceptual life history model showing
 1974 spatiotemporally-explicit hypotheses by life stage related to factors (covariates) affecting
 1975 survival.
 1976

1977 See TableA1_Stage_Hypotheses.pdf
 1978

1979
 1980
 1981
 1982
 1983

1984 TABLE A2: Models with $\Delta AICc < 2.0$ for each stage (pre-pawning female conditioning
1985 to age-0 pelagic juveniles) in the Pacific hake (*Merluccius productus*) conceptual life
1986 history model, all stages combined, and all stages with predator, prey, and climate
1987 indices.
1988
1989 See TableA2_R_Table_Delta2.hake_all_stages_models_pre_to_age0_FO_Revision.xlsx

TABLE A1: Pacific hake (*Merluccius productus*) conceptual life history model showing spatiotemporally-explicit hypotheses by life stage related to factors (covariates) affecting survival.

Ho Number	Life-history stage	Time period	Hypothesis	Stage	Covariates	Depth	Longitudinal extent	Latitudinal extent	Source
H1	Preconditioning	Apr - Oct (Year 0)	(H1) Higher temperature increases food demand resulting in lower egg production, egg quality, or probability of spawning and lowers recruitment	TEMP _{pre}	Mean temperature	50 - 350 m	Shelf break, between 100 - 2000 m isobaths	42° - 47°N	ROMS
H2			(H2) As (H1), but degree days, not mean temperature	DD _{pre}	Degree days	50 - 350 m	Shelf break, between 100 - 2000 m isobaths	42° - 47°N	ROMS
H3			(H3) Higher coastal upwelling leads to increased productivity, better condition, higher egg production, egg quality, or probability of spawning and increases recruitment	UW _{pre,c}	Coastal upwelling (CUT1)	Base of mixed layer		41.5° - 47.5°N	Jacox et al. (2018), https://oceanview.pfeg.noaa.gov
H4			(H4) As (H3), but biologically effective upwelling	UW _{pre,b}	Biologically effective upwelling (BEUT1)	Base of mixed layer	0 - 75 km offshore	41.5° - 47.5°N	Jacox et al. (2018), https://oceanview.pfeg.noaa.gov
H5			(H5) Food availability affects energy allocation to reproduction with higher recruitment when more prey are available during the preconditioning period	PRE _{pre,her} PRE _{pre,juvhake}	Index of age-0 and age-1 Pacific hake biomass, and age-2 Pacific herring biomass				Stock assessments
H6			(H6) Timing of availability of food affects energy allocation to reproduction with higher recruitment when more prey are available during the preconditioning period	SPTR _{pre}	Mean date of the spring transition from downwelling-favorable southerly winds to upwelling-favorable northerly winds		125°W	42°N (West of OR/CA border) 45°N (West of Siletz Bay, OR) 48°N (West of La Push, WA)	CBR Mean Method, Van Holmes (2007), http://www.cbr.washington.edu/status/trans
H7	Spawning	Jan - Mar	(H7) Temperature acts as a spawning cue with fish less likely to spawn at high temperature resulting in lower recruitment	TEMP _{spawn}	Mean temperature	130 - 500 m	Shelf break, between 100 - 2000 m isobaths	31° - 36°N	ROMS
H8			(H8) As (H7), but degree days, not mean temperature	DD _{spawn}	Degree days	130 - 500 m	Shelf break, between 100 - 2000 m isobaths	31° - 36°N	ROMS
H9	Eggs	Jan - Mar	(H9) Eggs aggregate at base of mixed layer so Mixed Layer Depth may limit how far they rise in the water column affecting later transport	MLD _{eggs}	Mean mixed layer depth (m)		Shelf break, between 100 - 2000 m isobaths	31° - 36°N	ROMS
H10			(H10) Transport to settlement habitat affects recruitment (transport varies with latitude)	CST _{eggs,s} CST _{eggs,n}	Net cross-shelf transport	40 - 60 m	Shelf break, between 100 - 2000 m isobaths	31° - 34.5°N 34.5° - 36°N	ROMS
H11			(H11) Increased northward advection away from juvenile nursery areas decreases recruitment	AST _{eggs}	Net alongshore transport	40 - 60 m	Shelf break, between 100 - 2000 m isobaths	31° - 36°N	ROMS
H12			(H12) Increased northward advection away from juvenile nursery areas decreases recruitment	PU _{eggs}	Strength of the poleward undercurrent	75 - 275 m	Coast to 275 m isobath	32.5° - 33.5°N	ROMS
H13			(H13) Growth/Predation hypothesis: growth rate is faster in warm water leading to reduced time vulnerable to predators	DD _{eggs}	Degree days	40 - 60 m	Shelf break, between 100 - 2000 m isobaths	31° - 36°N	ROMS
H14	Yolk-sac larvae	Jan - Apr	(H14) Larvae aggregate at base of mixed layer so Mixed Layer Depth may limit how far they rise in the water column affecting later transport	MLD _{yolk}	Mean mixed layer depth (m)		Shelf break, between 100 - 2000 m isobaths	31° - 36°N	ROMS
H15			(H15) Transport to settlement habitat affects recruitment (transport varies with latitude)	CST _{yolk,s} CST _{yolk,n}	Net cross-shelf transport	50 - 100 m	Shelf break, between 100 - 2000 m isobaths	31° - 34.5°N 34.5° - 36°N	ROMS
H16			(H16) Increased northward advection away from juvenile nursery areas decreases recruitment	AST _{yolk}	Net alongshore transport				ROMS
H17			(H17) Increased northward advection away from juvenile nursery areas decreases recruitment	PU _{yolk}	Strength of the poleward undercurrent	75 - 275 m	Coast to 275 m isobath	32.5° - 33.5°N	ROMS
H18			(H18) Growth/Predation hypothesis: growth rate is faster in warm water leading to reduced time vulnerable to predators	DD _{yolk}	Degree days	50 - 100 m		31° - 36°N	ROMS
H19	First-feeding larvae	Feb - May	(H19) Larvae aggregate at base of mixed layer so Mixed Layer Depth may limit how far they rise in the water column affecting later transport	MLD _{larv}	Mean mixed layer depth (m)		Shelf break, between 100 - 2000 m isobaths	31° - 36°N	ROMS
H20			(H20) Transport to settlement habitat affects recruitment (transport varies with latitude)	CST _{larv,s} CST _{larv,n}	Net cross-shelf transport	50 - 200 m	Shelf break, between 100 - 2000 m isobaths	31° - 34.5°N 34.5° - 36°N	ROMS
H21			(H21) North to south transport brings northern zooplankton and leads to higher survival and recruitment, Transport to settlement habitat affects recruitment	AST _{larv}	Net alongshore transport	50 - 200 m	Shelf break, between 100 - 2000 m isobaths	31° - 36°N	ROMS

TABLE A1 (cont'd): Pacific hake (<i>Merluccius productus</i>) conceptual life history model showing spatiotemporally-explicit hypotheses by life stage related to factors (covariates) affecting survival.									
H ₀ Number	Life-history stage	Time period	Hypothesis	Stage	Covariates	Depth	Longitudinal extent	Latitudinal extent	Source
H22	First-feeding larvae	Feb - May	(H22) Increased northward advection away from juvenile nursery areas decreases recruitment	PU _{larv}	Strength of the poleward undercurrent	75 - 275 m	Coast to 275 m isobath	32.5° - 33.5°N	
H23			(H23) Higher coastal upwelling leads to increased productivity, better condition, higher survival and increased recruitment	UW _{larv,cs} UW _{larv,cn}	Coastal upwelling (CUT1)	base of mixed layer	0 - 75 km offshore	30.5° - 34.5°N 34.5° - 36.5°N	Jacox et al. (2018), https://oceanview.pfeg.noaa.gov/
H24			(H24) As (H23), but biologically effective upwelling	UW _{larv,bs} UW _{larv,bn}	Biologically effective upwelling (BEUT1)	base of mixed layer	0 - 75 km offshore	30.5° - 34.5°N 34.5° - 36.5°N	Jacox et al. (2018), https://oceanview.pfeg.noaa.gov/
H25			(H25) Growth/Predation hypothesis: growth rate	DD _{larv}	Degree days	50 - 200 m	Shelf break, between 100 - 2000 m isobaths	31° - 36°N	ROMS
H26			(H26) Higher zooplankton abundance leads to higher survival and recruitment	PREY _{larv,zp}	Index of copepod abundance	0 - 210 m	117.4 - 121.9°W	31.5° - 34.5°N	Zooplankton Database, Scripps Institute of Oceanography https://oceaninformatics.ucsd.edu/zoodb/secure/login.php
H27			(H27) Critical period hypothesis: more frequent storm events lead to poorer feeding conditions,	STORM _{larv}	Mean number of storm events		Coast to 126°W	28° - 36°N	Turley and Rykaczewski (2019) NOAA National Centers for Environmental Prediction Climate Forecast System Reanalysis model (CFSR, Saha et al., 2010)
H28			(H28) Critical period hypothesis: extended storm events lead to poorer feeding conditions, lower	STORM _{larv}	Mean duration of storm events		Coast to 126°W	28° - 36°N	Turley and Rykaczewski (2019), CFSR, Saha et al. (2010)
H29			(H29) Critical period hypothesis: fewer days between storm events lead to poorer feeding	STORM _{larv}	Mean number of days between storm events		Coast to 126°W	28° - 36°N	Turley and Rykaczewski (2019), CFSR, Saha et al. (2010)
H30			(H30) Critical period hypothesis: more frequent calm events lead to better feeding conditions,	CALM _{larv}	Mean number of calm events		Coast to 126°W	28° - 36°N	Turley and Rykaczewski (2019), CFSR, Saha et al. (2010)
H31			(H31) Critical period hypothesis: extended periods of calm lead to poorer feeding conditions,	CALM _{larv}	Mean duration of calm events		Coast to 126°W	28° - 36°N	Turley and Rykaczewski (2019), CFSR, Saha et al. (2010)
H32			(H32) Critical period hypothesis: shorter intervals between calm events lead to better feeding	CALM _{larv}	Mean number of days between calm events		Coast to 126°W	28° - 36°N	Turley and Rykaczewski (2019), CFSR, Saha et al. (2010)
H33	Late larvae	Mar - Jun	(H33) Larvae aggregate at base of mixed layer so Mixed Layer Depth may limit how far they rise in the water column affecting later transport	ML _{late,larv}	Mean location of mixed layer depth (m)		Shelf break, between 100 - 2000 m isobaths	31° - 37°N	ROMS
H34			(H34) Transport to settlement habitat affects recruitment (transport varies with latitude)	CST _{late,larv,s} CST _{late,larv,n}	Net cross-shelf transport	50 - 300 m	Shelf break, between 100 - 2000 m isobaths	31° - 34.5°N 34.5° - 37°N	ROMS
H35			(H35) North to south transport brings northern zooplankton and leads to higher survival and recruitment, Transport to settlement habitat affects recruitment	AST _{late,larv}	Net alongshore transport	50 - 300 m	Shelf break, between 100 - 2000 m isobaths	31° - 37°N	ROMS
H36			(H36) Increased northward advection away from juvenile nursery areas decreases recruitment	PU _{late,larv}	Strength of the poleward undercurrent	75 - 275 m	Coast to 275 m isobath	33.5° - 34.5°N	ROMS
H37			(H37) Higher coastal upwelling leads to increased productivity, better condition, higher survival and increased recruitment	UW _{late,larv,cs} UW _{late,larv,cn}	Coastal upwelling (CUT1)	base of mixed layer	0 - 75 km offshore	30.5° - 34.5°N 34.5° - 37.5°N	Jacox et al. (2018), https://oceanview.pfeg.noaa.gov
H38			(H38) As (H37), but biologically effective upwelling	UW _{late,larv,bs} UW _{late,larv,bn}	Biologically effective upwelling (BEUT1)	base of mixed layer	0 - 75 km offshore	30.5° - 34.5°N 34.5° - 37.5°N	Jacox et al. (2018), https://oceanview.pfeg.noaa.gov
H39			(H39) Growth/Predation hypothesis: growth rate is faster in warm water leading to reduced time vulnerable to predators	DD _{late,larv}	Degree days	50 - 300 m	Shelf break, between 100 - 2000 m isobaths	31° - 37°N	ROMS
H40			(H40) Timing of availability of food affects condition, leading to higher survival and increased recruitment	SPTR _{late,larv}	Mean date of the spring transition from downwelling-favorable southerly winds to upwelling-favorable northerly winds		125°W	42°N (West of OR/CA border) 45°N (West of Siletz Bay, OR) 48°N (West of La Push, WA)	CBR Mean Method, Van Holmes (2007) http://www.cbr.washington.edu/status/trans
H41			(H41) Higher prey abundance leads to higher survival and recruitment	PREY _{late,larv,zp} PREY _{late,larv,eup}	Index of copepod abundance Index of euphausiid abundance	0 - 210 m 0 - 210 m	117.4 - 121.9°W 117.3 - 125.0°W	31.5° - 34.5°N 29.9° - 35.1°N	Zooplankton Database, Scripps Institute of Oceanography (https://oceaninformatics.ucsd.edu/zoodb/secure/login.php) Brinton and Townsend Euphausiid Database, SIO https://oceaninformatics.ucsd.edu/euphausiid/secure/login.php

TABLE A1 (cont'd): Pacific hake (*Merluccius productus*) conceptual life history model showing spatiotemporally-explicit hypotheses by life stage related to factors (covariates) affecting survival.

H ₀ Number	Life-history stage	Time period	Hypothesis	Stage	Covariates	Depth	Longitudinal extent	Latitudinal extent	Source
H42	Pelagic juveniles (age-0)	Apr - Sep	(H42) Transport to settlement habitat affects recruitment (transport varies with latitude)	CST _{age0,s} CST _{age0,n}	Net cross-shelf transport	0 - 50 m	inshore of 200 m isobath	31° - 34.5°N 34.5° - 38°N	ROMS
H43			(H43) North to south transport brings northern zooplankton and leads to higher survival and recruitment, Transport to settlement habitat affects recruitment	AST _{age0}	Net alongshore transport	0 - 50 m	inshore of 200 m isobath	31° - 38°N	ROMS
H44			(H44) Higher coastal upwelling leads to increased productivity, better condition, higher survival and increased recruitment (upwelling varies with latitude)	UW _{age0,cs} UW _{age0,cn}	Coastal upwelling (CUTI)	base of mixed layer	0 - 75 km offshore	30.5° - 34.5°N 34.5° - 38.5°N	Jacox et al. (2018), https://oceanview.pfeg.noaa.gov
H45			(H45) As (H44), but biologically effective upwelling	UW _{age0,bs} UW _{age0,bn}	Biologically effective upwelling (BEUTI)	base of mixed layer	0 - 75 km offshore	30.5° - 34.5°N 34.5° - 38.5°N	Jacox et al. (2018), https://oceanview.pfeg.noaa.gov
H46			(H46) Growth/Predation hypothesis: growth rate is faster in warm water leading to reduced time vulnerable to predators	DD _{age0}	Degree days	0 - 50 m	inshore of 200 m isobath	31° - 38°N	ROMS
H47			(H47) Timing of availability of food affects condition, leading to higher survival and increased recruitment	SPTR _{age0}	Mean date of the spring transition from downwelling-favorable southerly winds to upwelling-favorable northerly winds		125°W	42°N (West of OR/CA border) 45°N (West of Siletz Bay, OR) 48°N (West of La Push, WA)	CBR Mean Method, Van Holmes (2007) http://www.cbr.washington.edu/status/trans
H48			(H48) Increased food availability leads to better feeding conditions, leading to higher survival and recruitment	PREY _{age0,eup}	Index of euphausiid abundance	0 - 210 m	117.3 - 125.0°W	29.9° - 35.1°N	Brinton and Townsend Euphausiid Database, SIO https://oceaninformatics.ucsd.edu/euphausiid/secure/login.php
H49			(H49) Higher predation leads to lower survival and recruitment	PRED _{age0,age1hake} PRED _{age0,aff} PRED _{age0,csi}	Index of age-1 Pacific hake biomass, arrowtooth flounder biomass, California sea lion pup counts				Stock assessments, Laake et al. (2017)
H50	Preconditioning Egg to late larvae First feeding larvae to age-0	Jan - Apr May - Sep Jan - Apr May - Sep	(H50) Sea surface height as an indicator of basin-scale processes	SSH _{pre,JA,s} SSH _{pre,JA,c} SSH _{pre,MS,c} SSH _{pre,MS,n} SSH _{LA,s} SSH _{LA,c} SSH _{MS,s} SSH _{MS,c}	Sea surface height	Surface	0 - 30 km offshore	31° - 34.5°N 34.5° - 42.5°N 34.5° - 42.5°N 42.5° - 47°N 31° - 34.5°N 34.5° - 42.5°N 31° - 34.5°N 34.5° - 42.5°N	ROMS
H51	Preconditioning First feeding larvae to age-0 Late larvae to age-0	Jan - Apr May - Sep Jan - Apr May - Sep	(H51) Eddy kinetic energy as a proxy for the intensity of mesoscale turbulence - higher EKE, with more meanders, fronts, and eddies, leads to better feeding conditions, higher survival and recruitment	EKE _{pre,JA,s} EKE _{pre,JA,c} EKE _{pre,MS,c} EKE _{pre,MS,n} EKE _{LA,s} EKE _{LA,c} EKE _{MS,s} EKE _{MS,c}	Eddy kinetic energy	Surface	0 - 30 km offshore	34.5° - 42.5°N 42.5° - 47°N 34.5° - 42.5°N 42.5° - 47°N 31° - 34.5°N 34.5° - 42.5°N 31° - 34.5°N 34.5° - 42.5°N	ROMS
H52	Preconditioning	Apr - Sep Jan - Apr Apr - Sep	(H52) Pacific Decadal Oscillation as an indicator of basin-scale processes; negative phase linked to higher productivity, better feeding conditions, better condition, higher survival and recruitment	PDO _{pre} PDO _{JA} PDO _{AS}	Pacific Decadal Oscillation				Mantua (1999), http://research.jisao.washington.edu/pdo/
H53	Preconditioning	Apr - Sep Jan - Apr Apr - Sep	(H53) North Pacific Gyre Oscillation as an indicator of basin-scale processes; positive phase linked to higher nutrient concentrations, higher productivity, better feeding conditions, better condition, higher survival and recruitment	NPGO _{pre} NPGO _{JA} NPGO _{AS}	North Pacific Gyre Oscillation				Di Lorenzo et al. (2008), http://www.o3d.org/npgo/
H54	Preconditioning First-feeding larvae to age-0		(H54) More northward shifted bifurcation of the North Pacific Current leads to increased transport of enriched subarctic waters to the south, higher productivity, better feeding conditions, better condition, higher survival and recruitment	BI _{pre} BI	Bifurcation Index				Malick et al. (2017)